Higgs-vector boson CP studies

October 28th, 2020

Online conference
HIGGS 2020
October 26-30

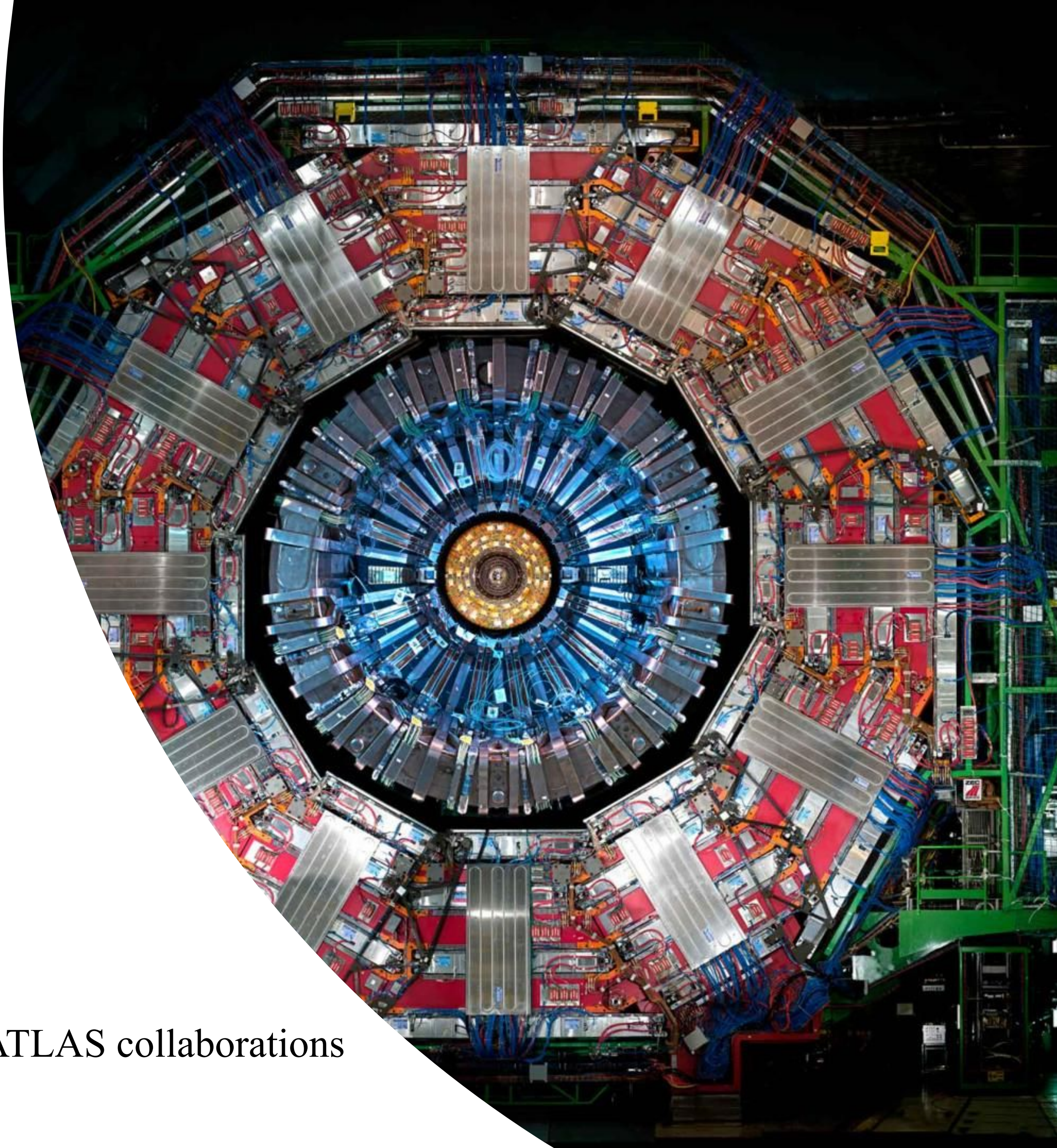

Doyeong Kim 김 도 영

on behalf of the CMS and ATLAS collaborations

Introduction

What we know

- Spin-parity quantum number of Higgs boson consistent with standard model (SM) expectation (i.e. $J^{cp} = 0^{++}$)

What we don't know

- Does Higgs sector have a new source of charge conjugation parity (CP) violation?
  - Any observed CP violation would indicate beyond standard model (BSM)

Basic idea

- Different spin-parity assignments restrict the allowed types of interactions manifesting in the kinematics of
  1) Particles produced in association with Higgs boson → **CP in production**
  2) Decay products of the Higgs boson → **CP in decay**

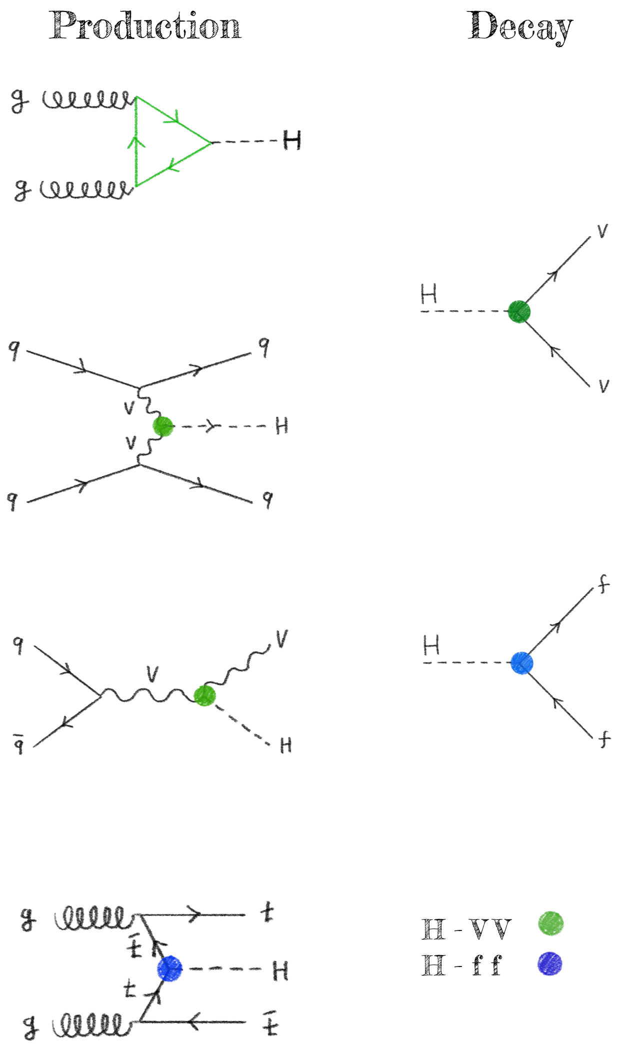

Overview of CP studies using H-VV vertices

Motivation

How to probe H-VV vertices?

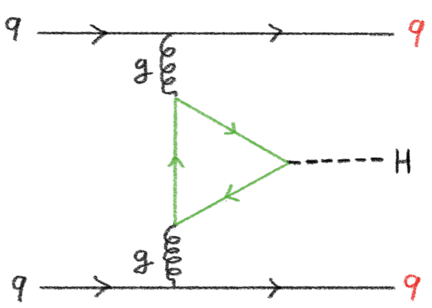

Second order ggH production

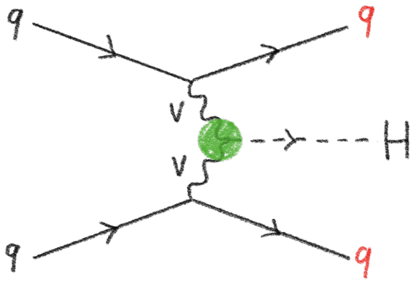

VBF production

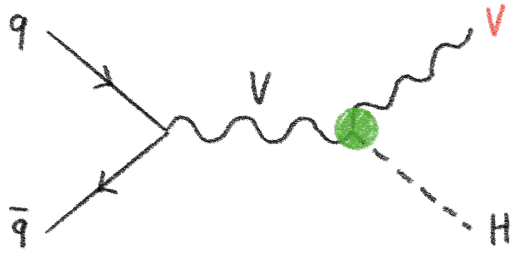

VH production

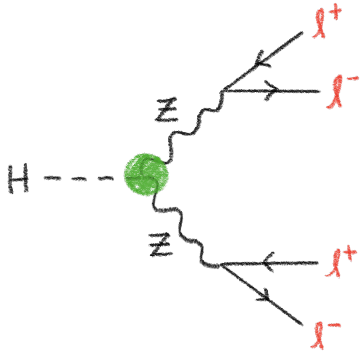

H→ZZ→4*l* decay

Where *l* is *e* or *μ*

- Decay channels with clean signature (**H→ZZ→4*l*, H→WW*→(eνμν)jj**) can easily employ second order ggH production
- Using VBF production: **H→ττ** is essential due to its high branching ratio
- Using H→VV decay: **H→ZZ→4*l*** is the most sensitive decay channel due to its clean signature
- Contribution of VH production is small but non-negligible in H→ZZ→4*l* analyses

Parametrization

Generic spin-0 H-VV scattering amplitude

tree-level SM-like | CP-even anomalous couplings | CP-odd anomalous coupling

$$\mathcal{A}(\mathrm{HVV}) \sim \left[a_1^{\mathrm{VV}} + \frac{\kappa_1^{\mathrm{VV}} q_1^2 + \kappa_2^{\mathrm{VV}} q_2^2}{\left(\Lambda_1^{\mathrm{VV}}\right)^2} \right] m_{\mathrm{V1}}^2 \epsilon_{\mathrm{V1}}^* \epsilon_{\mathrm{V2}}^* + a_2^{\mathrm{VV}} f_{\mu\nu}^{*(1)} f^{*(2)\mu\nu} + a_3^{\mathrm{VV}} f_{\mu\nu}^{*(1)} \tilde{f}^{*(2)\mu\nu}$$

Where VV = ZZ, WW, Zγ, $\gamma\gamma$, gg

Considering gauge invariance, custodial symmetry and additional assumptions (**CMS-PAS-HIG-19-009**)

$a_i^{ZZ} = a_i^{WW}$, $\kappa_i^{ZZ}/(\Lambda_1^{ZZ})^2 = \kappa_i^{WW}/(\Lambda_1^{WW})^2$

Hereafter WW and ZZ superscript will be omitted

Seven couplings remain: **a_1, a_2, a_3, Λ_1, $\Lambda_1^{Z\gamma}$** , and **a_1^{ggH}, a_3^{ggH}**

SMEFT

$$\mathcal{L}_{\mathrm{EFT}} = \mathcal{L}_{\mathrm{SM}} + \sum_i \frac{C_i^{(d)}}{\Lambda^{(d-4)}} O_i^{(d)} \quad \text{for } d > 4$$

$C_i^{(d)}$: Wilson coefficients

Λ : scale of new physics

Only dimension-six operators are considered ($c_i = C_i^{(d=6)}/\Lambda^2$)

Recent Analyses in CMS and ATLAS

Various choices of SMEFT bases are possible to probe CP properties of Higgs boson

- Warsaw basis - self consistent at one loop (the most standard basis)
- Mass basis - mass eigenstates after electroweak symmetry breaking
- Higgs basis - independent couplings include single Higgs boson couplings to V, and f

	CMS	ATLAS
H→ZZ→4*l*	Full Run2 (137.1 fb^{-1}) [1] H-VV, H-ff anomalous couplings & EFT coefficients • Anomalous amplitude decomposition • SMEFT - Higgs basis	Full Run2 (139 fb^{-1}) [3] H-VV, H-ff • SMEFT - Warsaw basis
H→ττ	2016 Run2 (35.9 fb^{-1}) [2] H-VV anomalous couplings • Anomalous amplitude decomposition	2015+2016 Run2 (36.1 fb^{-1}) [4] H-VV anomalous couplings (CP odd only, target VBF) • SMEFT - Mass basis
H→WW →(eνμν)jj	-	2015+2016 Run2 (36.1 fb^{-1}) [8] H-VV anomalous couplings (CP odd only, target ggH) • SMEFT - Mass basis

New wrt preceding analyses ([5] and [6])

Comprehensive Goals (Categorization)

Goal #1
Sig. vs Bkg.

Targets production modes

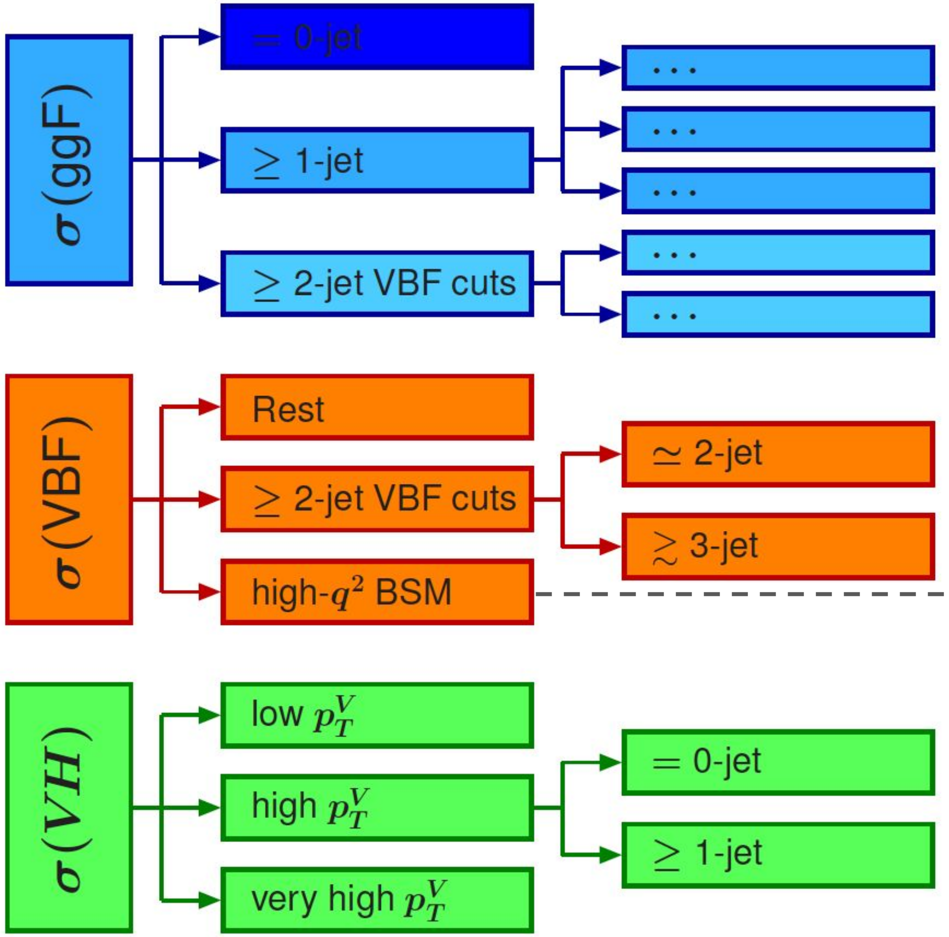

CERN report

Goal #2
SM vs BSM

Further optimization

STXS is designed to be sensitive to q^2 enhancement which is a general feature of higher-dim operators, including CP-odd and CP-even ones

Comprehensive Goals (Observables)

Goal #1
Sig. vs Bkg.

Goal #2
SM vs BSM

Eur. Phys. J. C 80 (2020) 957

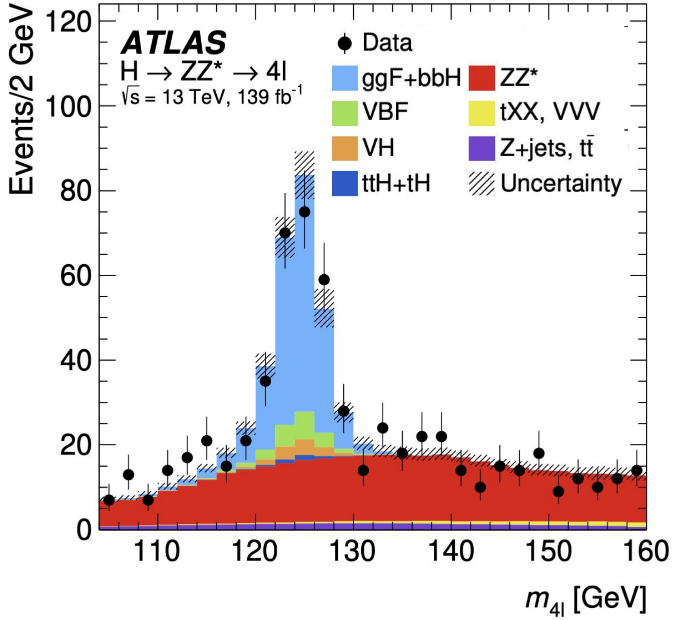

CERN report

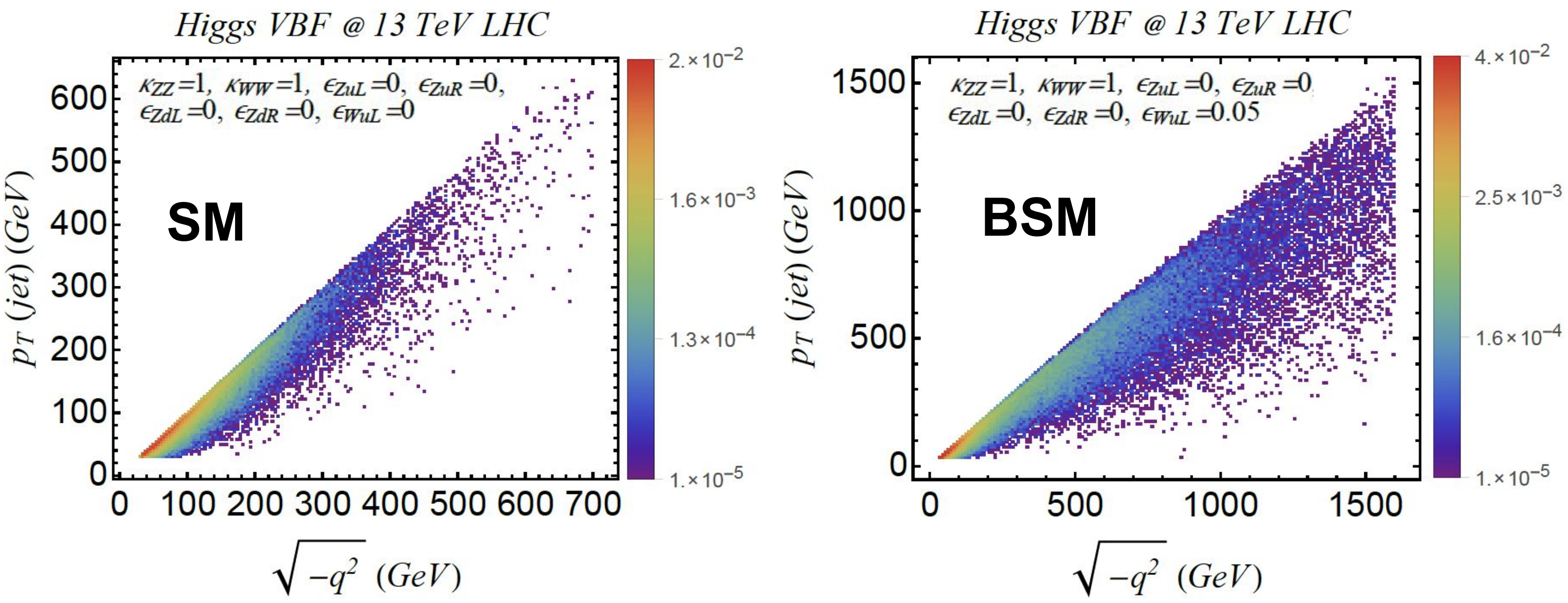

- **Goal #1:** Higgs boson invariant mass, Higgs boson transverse momentum, Di-jet invariant mass, ...
- **Goal #2:** Kinematics of two jets, Higgs boson decay products, …
- Many multivariable discriminants are employed to enhance the discriminating power

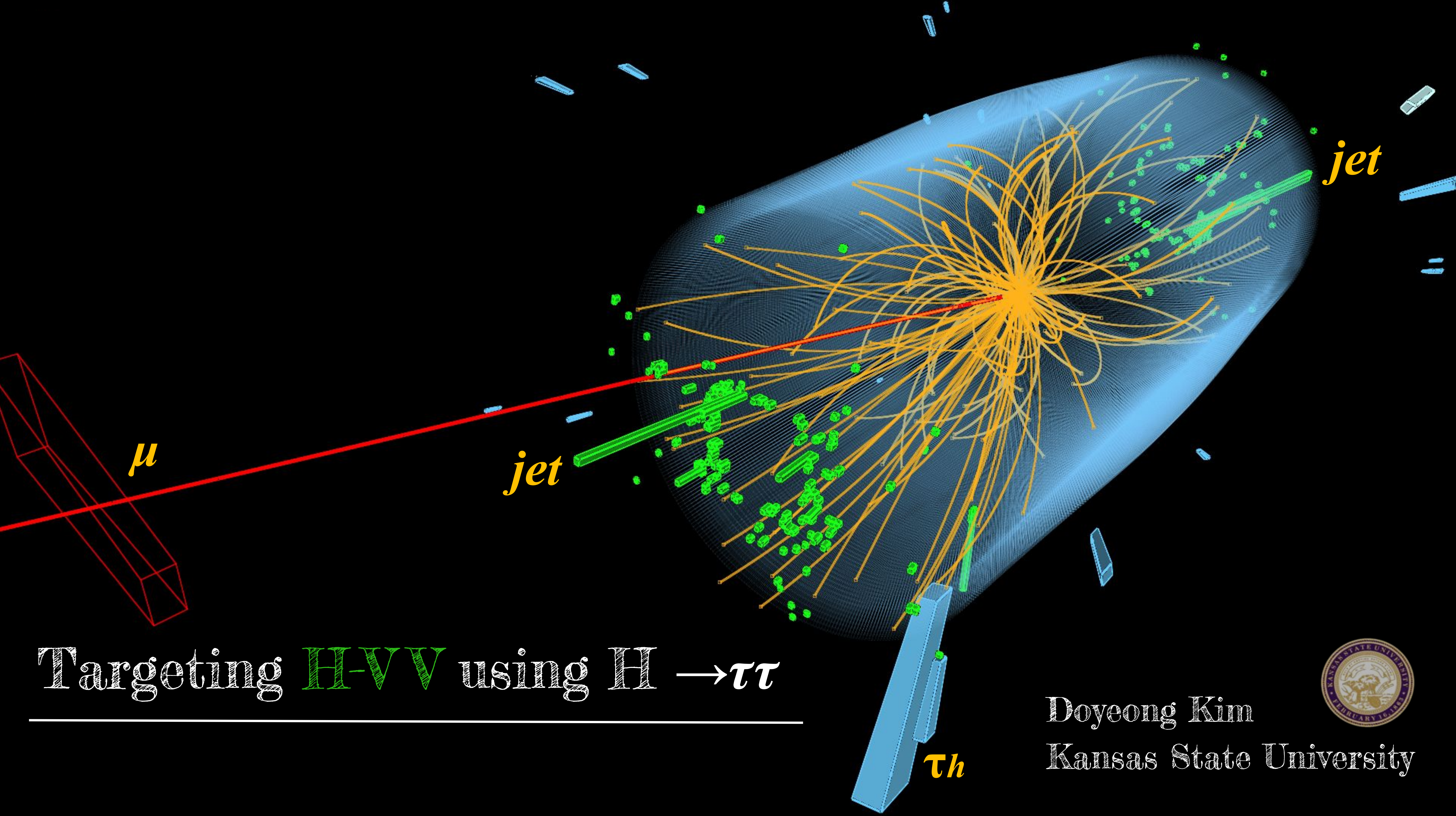

Targeting H-VV using H $\rightarrow\tau\tau$

Doyeong Kim
Kansas State University

Event Categorization (CMS)

VBF Category

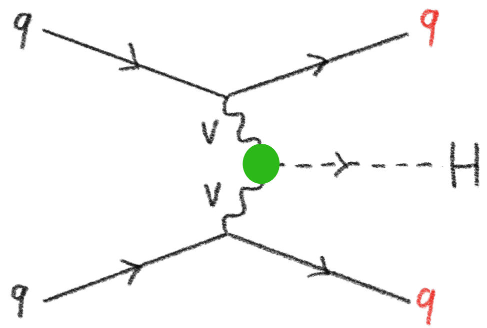

VBF

Two jets that have
large invariant mass and
large pseudorapidity separation

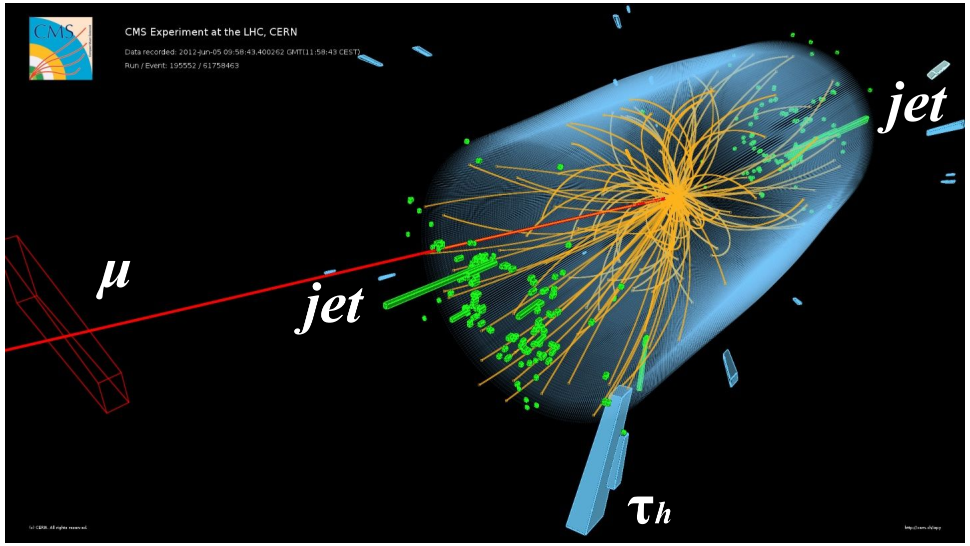

0 jet Category

- Constrain backgrounds

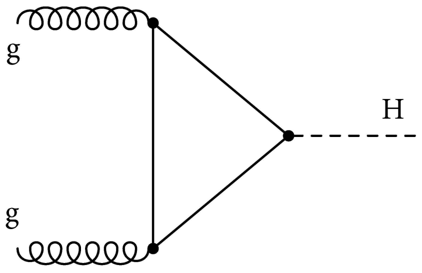

ggH + no jet

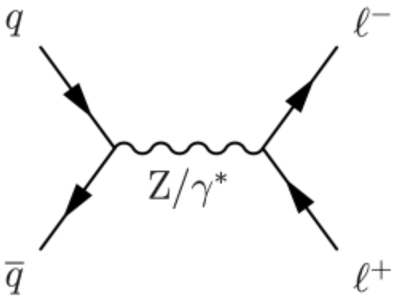

Background

Boosted Category

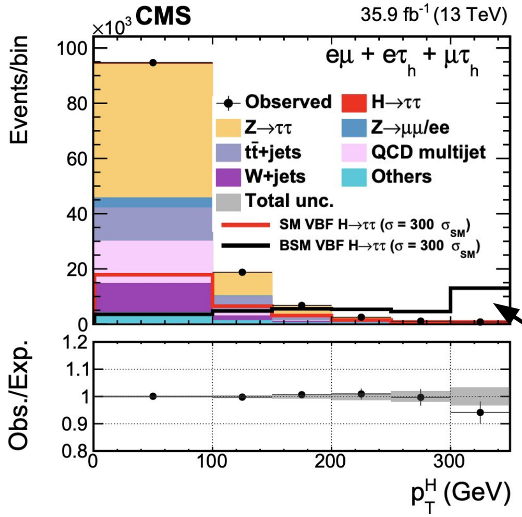

Large reconstructed Higgs boson transverse momentum

SM vs BSM
BSM harder Higgs p_T

Phys. Rev. D 100, 112002 | CMS H→ττ

CP studies using H-VV

Optimal Discriminants for VBF topology (ATLAS)

Phys. Lett. B 805 (2020) 135426 | ATLAS H→$\tau\tau$

- Same kinematics for VBF category as in CMS analysis:

  (at least 2 jets, large di-jet invariant mass, large pseudo rapidity separation)

- BDT score used to define signal regions

1) Sig vs Bkg
   $m_{\tau\tau}$
   $\Delta R_{\tau\tau}$
   :

2) VBF topology
   m_{jj}
   :

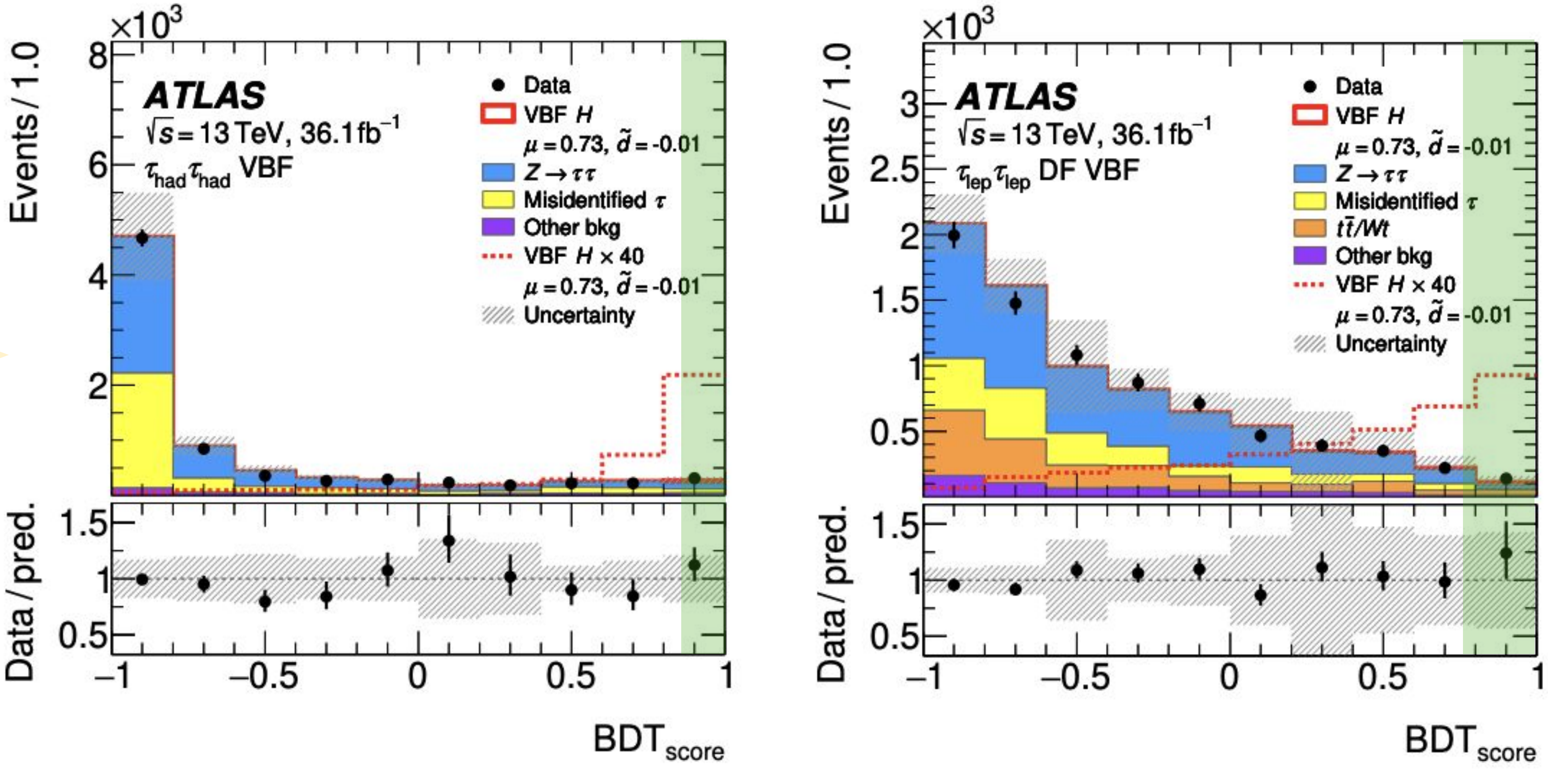

Optimal Discriminants for CP (CMS)

Phys. Rev. D 100, 112002 | CMS H→ττ

MELA (**M**atrix **E**lement **L**ikelihood **A**pproach)

- Use the full kinematics of the H-VV to calculate likelihood based on the matrix element
- Designed to reduce the number of observables to minimum, while retaining all essential information

MELA discriminants

✓ Easily constructed as the ratio of likelihoods
✓ Used to separate different hypothesis of signals or background

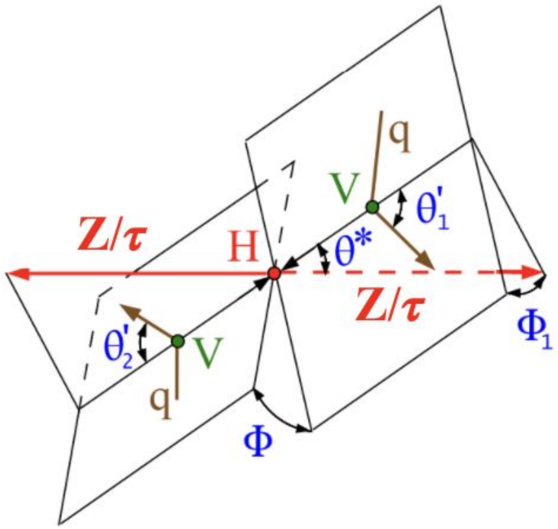

HVV in VBF
qq → VV(qq) →
H(qq) → ZZ or ττ (qq)

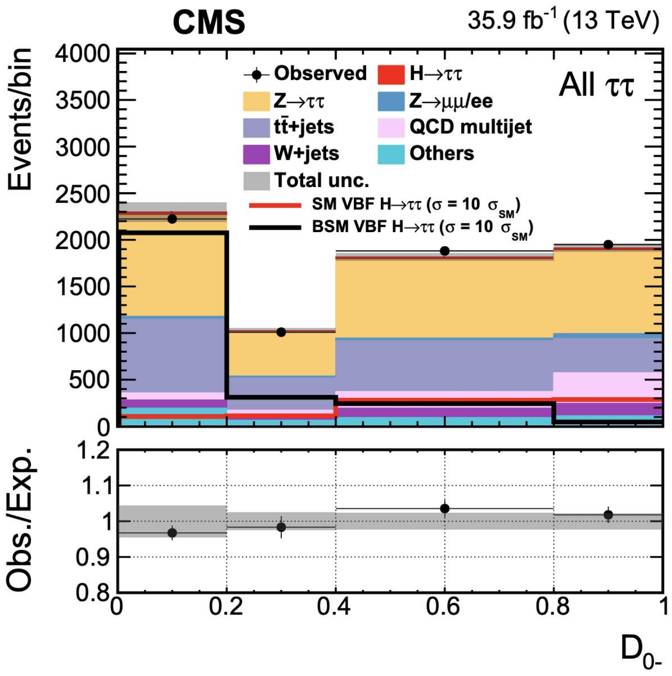

SM vs BSM

$$D_{BSM} = \frac{P_{SM}}{P_{SM} + P_{BSM}}$$

Optimal Discriminants for CP (ATLAS)

Phys. Lett. B 805 (2020) 135426 | ATLAS H→ττ

Optimal observable built using the matrix element

Using SMEFT represented in mass basis, CP violation in H-VV coupling described by a single parameter $\tilde{d}$

$$\mathcal{L}_{eff} = \mathcal{L}_{SM} + \mathcal{L}_{HVV}^{CP\text{-}odd}(\tilde{d}) + \mathcal{L}_{else}$$

$$\mathcal{M} = \mathcal{M}_{SM} + \tilde{d} \cdot \mathcal{M}_{CP\text{-odd}}$$

$$|\mathcal{M}|^2 = |\mathcal{M}_{SM}|^2 + \tilde{d} \cdot 2\,\mathrm{Re}(\mathcal{M}_{SM}^* \mathcal{M}_{CP\text{-odd}}) + \tilde{d}^2 \cdot |\mathcal{M}_{CP\text{-odd}}|^2$$

⬇

$$\mathcal{O}_{opt} = \frac{2\,\mathrm{Re}(\mathcal{M}_{SM}^* \mathcal{M}_{CP\text{-odd}})}{|\mathcal{M}_{SM}|^2}$$

$< \mathcal{O}_{opt} >$!= 0 would indicate CP-violation

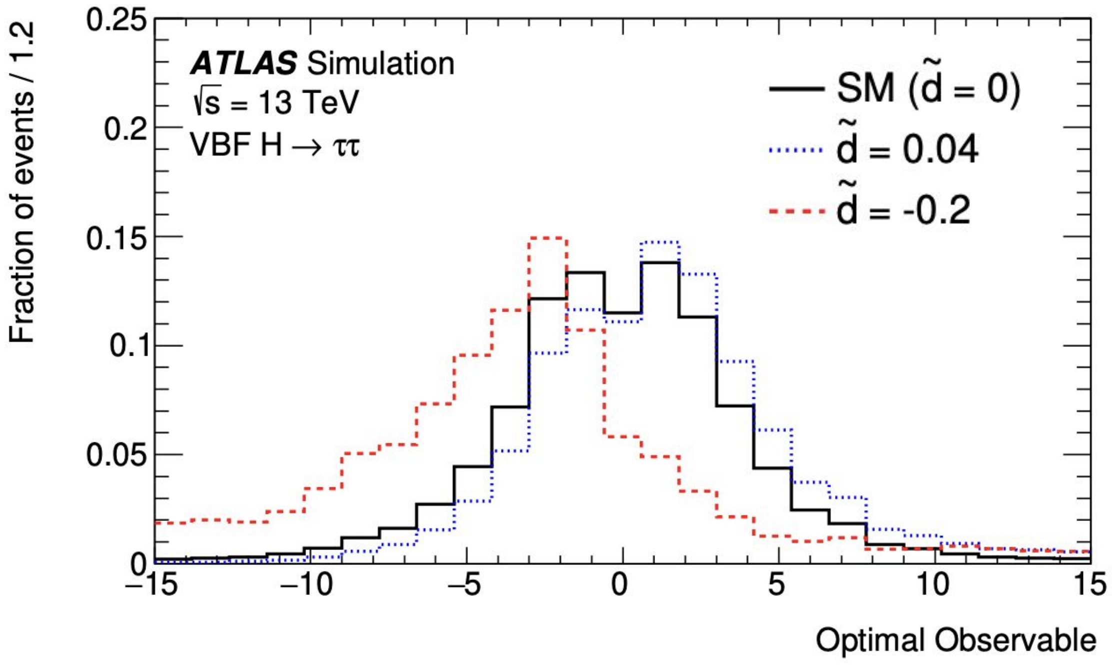

CP studies using H-VV

Constraint on CP-violating Parameters

Results from both experiments indicate no deviation from SM expectation

68% CL observed
[-0.27, 0.27]

95% CL observed
[-92, 14]

68% CL observed
[-0.93, 0.43]

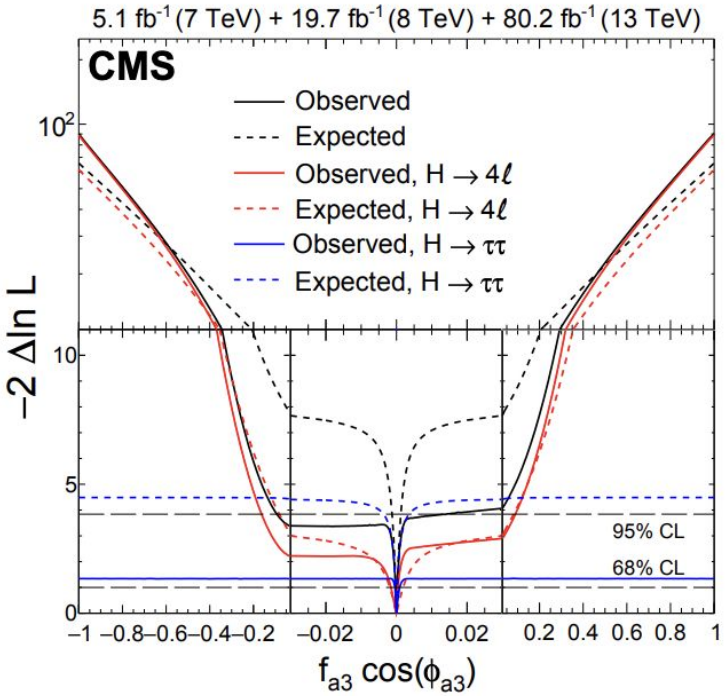

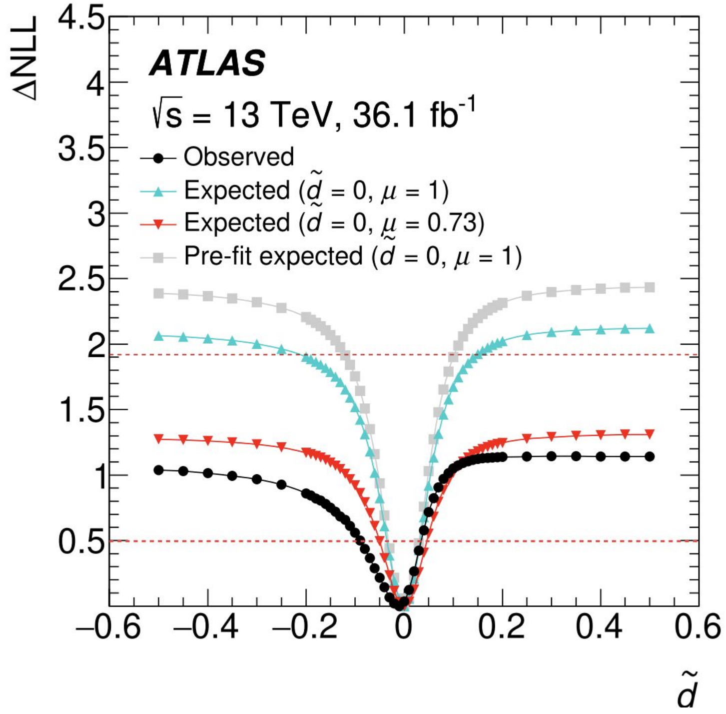

68% CL observed
[-0.09, 0.035]

Combination of H→$\tau\tau$ (Run2 2016) and
H→4l (Run1 2011, 2012 and Run2 2015, 2016, 2017)

Confidence intervals extracted for different μ

where $\mu = \frac{(\sigma \times BR)_{observed}}{(\sigma \times BR)_{expected}}$

Plots of CP-conserving parameters are in backup

Phys. Rev. D 100, 112002 | CMS H→$\tau\tau$

Phys. Lett. B 805 (2020) 135426 | ATLAS H→$\tau\tau$

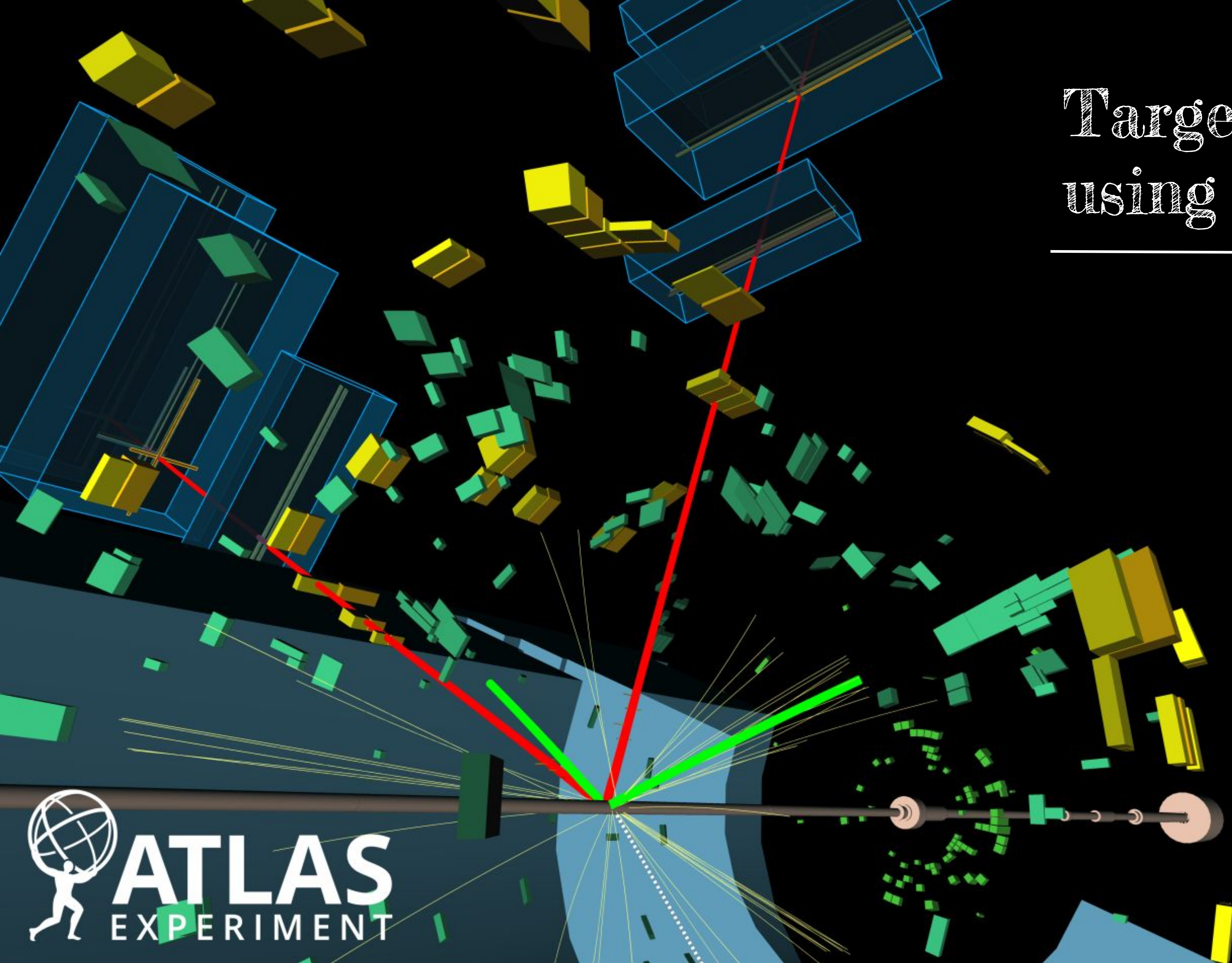

Targeting H-VV using H→ZZ→4l

Doyeong Kim
Kansas State University

STXS Based Event Categorization

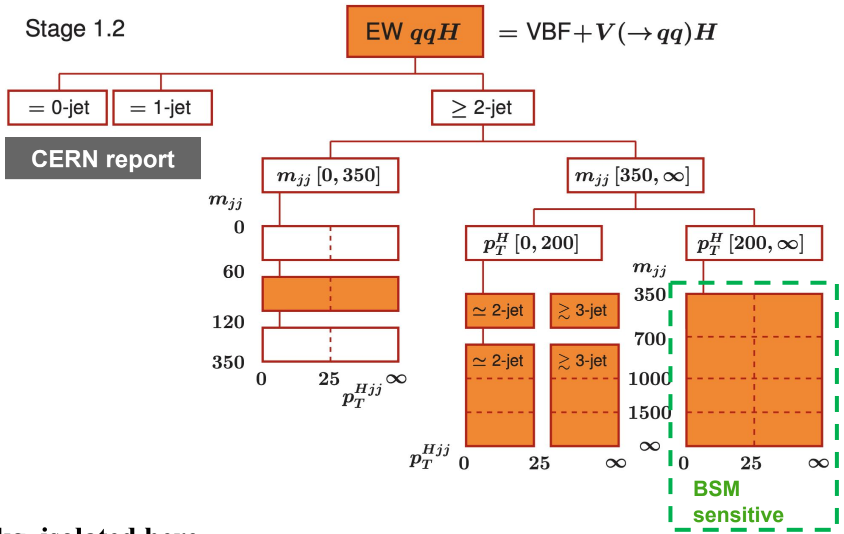

- Events are classified in categories targeting different Higgs production modes
- Some of bins in Simplified Template Cross Section (STXS) BSM sensitive phase space

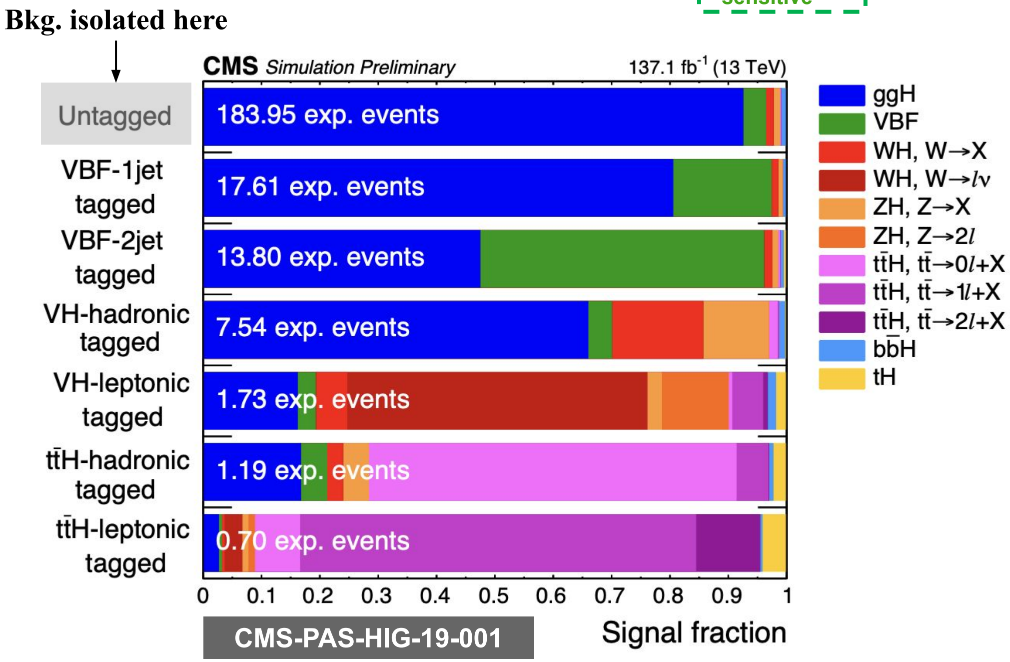

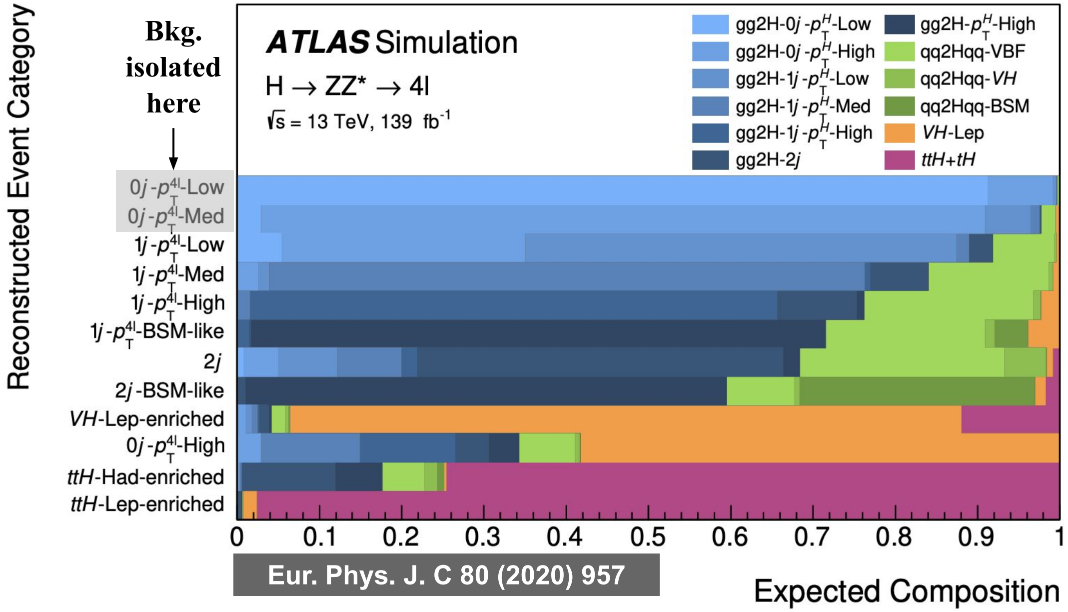

CP studies using **H-VV**

Optimal Discriminant for STXS (ATLAS)

Eur. Phys. J. C 80 (2020) 957 ATLAS H→ZZ→4l

- Multivariate neural network discriminants used as observables to increase the sensitivity of XS measurement
- Measured XS in STXS bins are interpreted using SMEFT represented in Warsaw basis

Limit set on this ratio

$$\sigma \propto |\mathcal{M}_{\mathrm{SMEFT}}|^2 = \left|\mathcal{M}_{\mathrm{SM}} + \sum_i \frac{C_i}{\Lambda^2}\mathcal{M}_i\right|^2$$

$C_i^{(d)}$: Wilson coefficients

Λ : scale of new physics

VBF 2jet bin

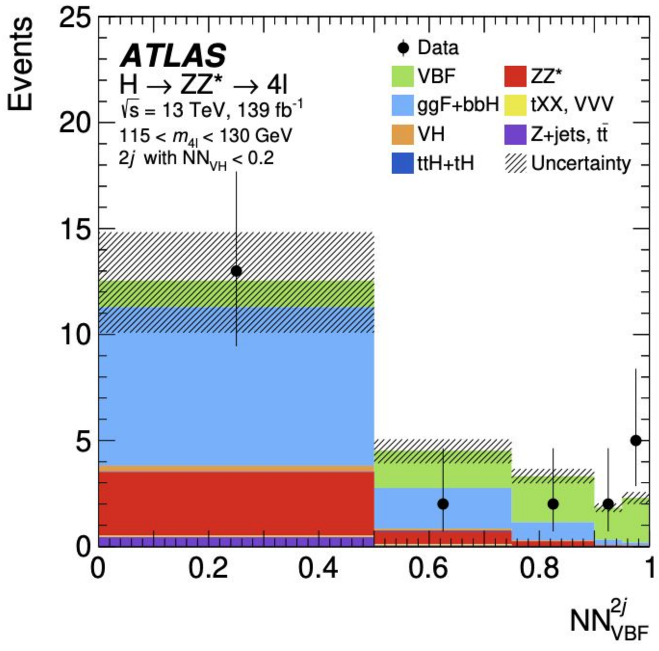

VH 2jet bin

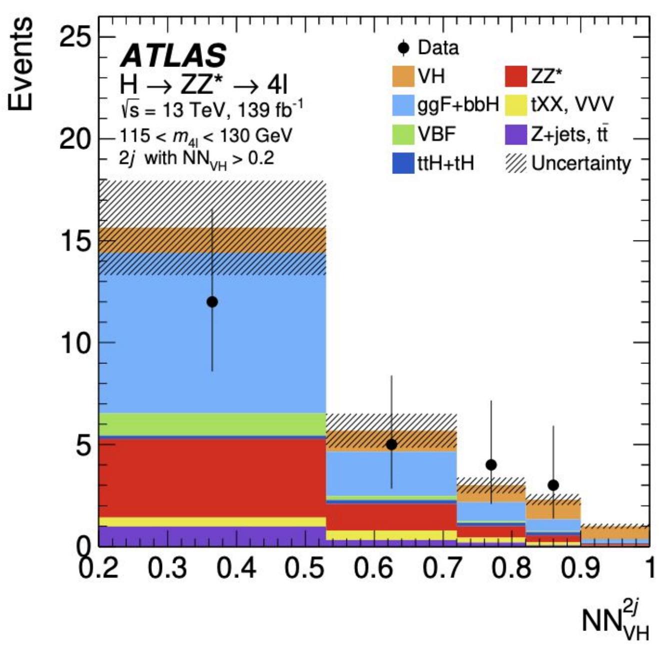

VBF 2jet BSM bin

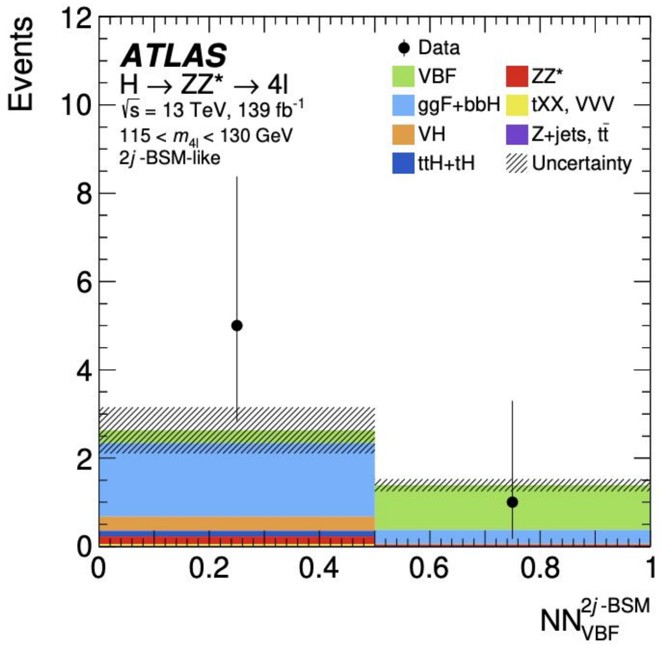

CP studies using H-VV

Optimal Discriminants for CP (CMS)

CMS-PAS-HIG-19-009 | CMS H→ZZ→4l

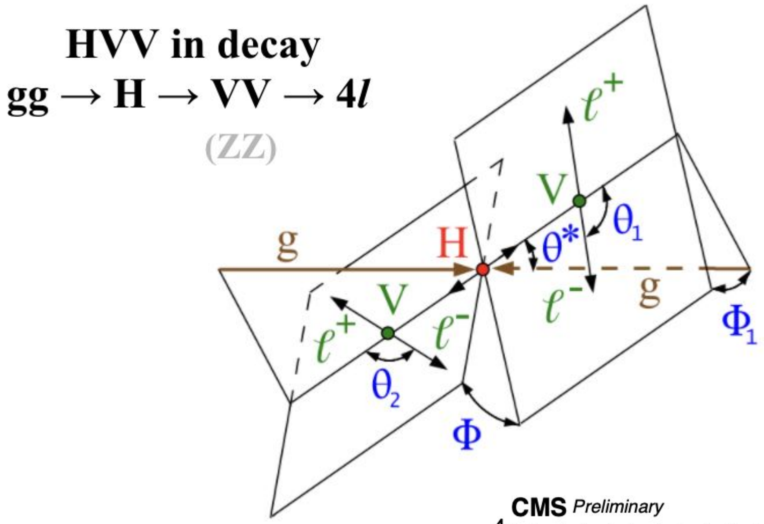

MELA discriminants are constructed using Higgs boson production and decay kinematics

Selections for this analysis come from CMS-HIG-19-001

$$D_{Bkg.} = \frac{P_{Bkg.}}{P_{Bkg.} + P_{Sig.}} \qquad D_{CP} = \frac{P_{int.} - (P_{SM} + P_{PS})}{P_{SM} + P_{PS}}$$

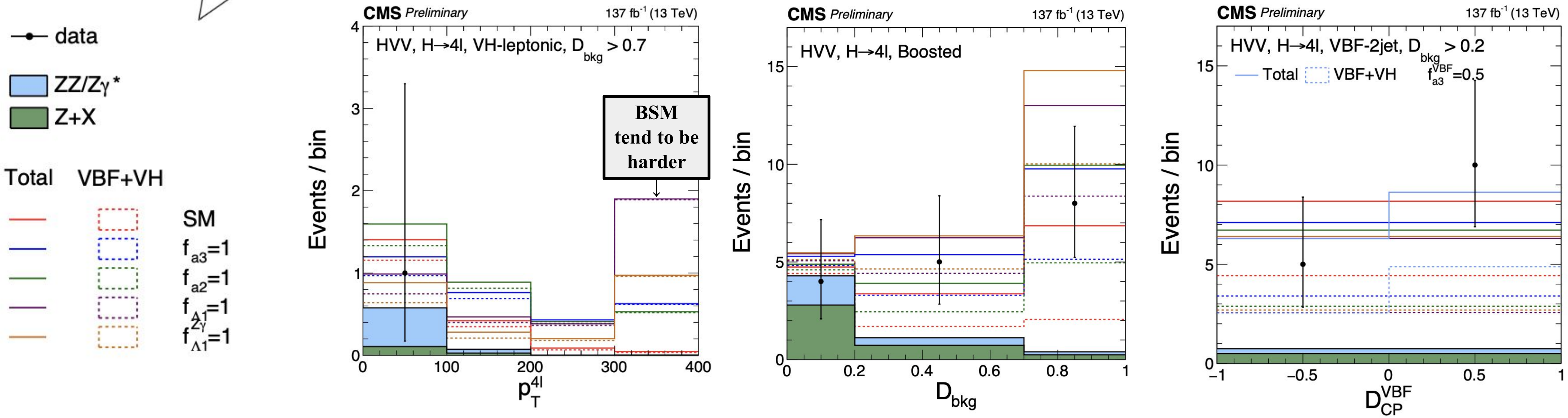

Constraint on CP-violating Parameters

Results from both experiments indicate no deviation from SM expectation

Best-fit : ±0.010
68% CL observed [-0.042, 0.034]
95% CL observed [-0.20, 0.20]

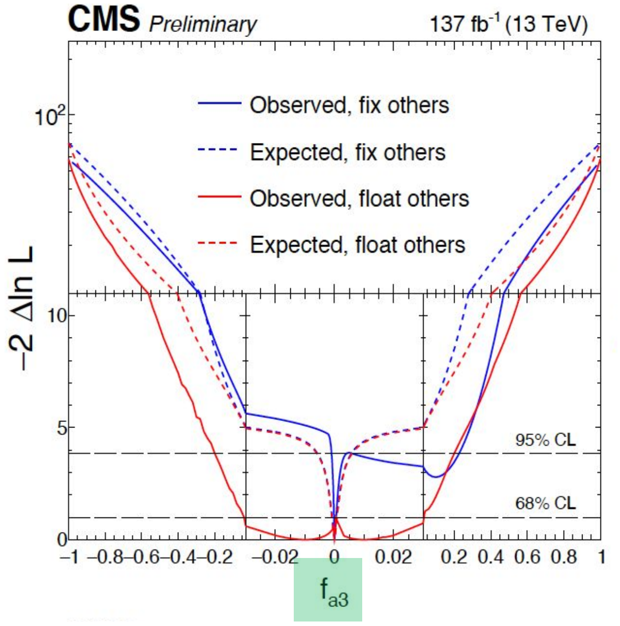

Best-fit : -0.53 -0.47/+0.51
68% CL observed [-1, 1]

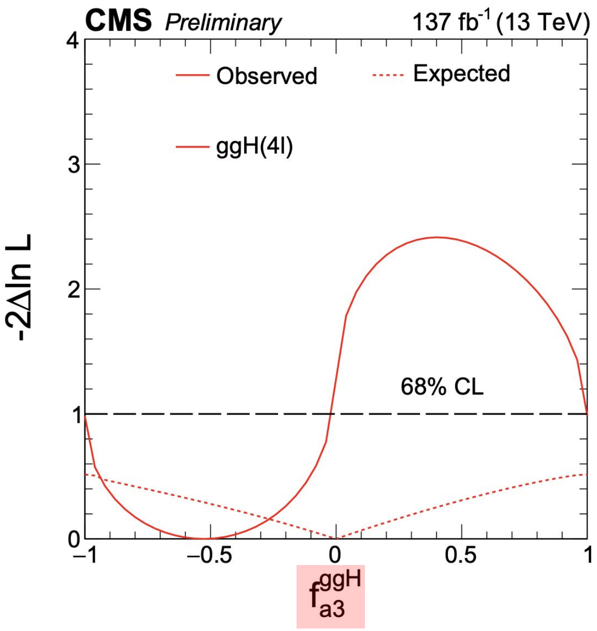

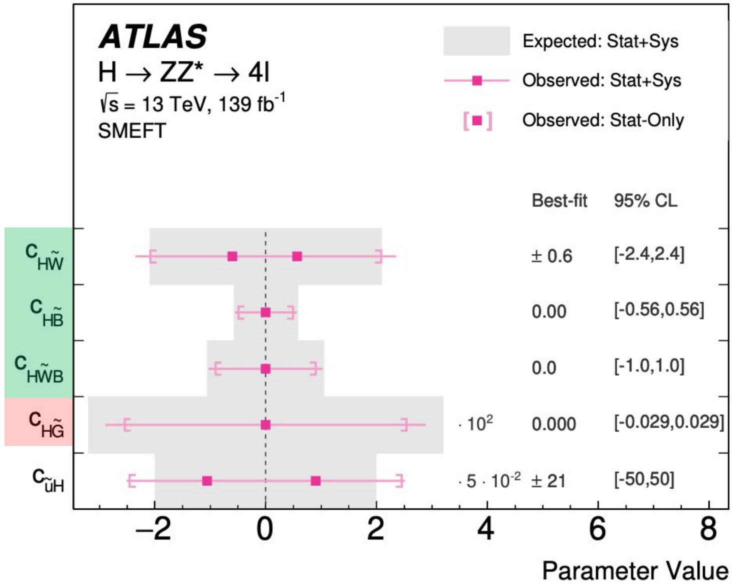

CMS-PAS-HIG-19-009 | CMS H→ZZ→4l

Eur. Phys. J. C 80 (2020) 957 | ATLAS H→ZZ→4l

Targeting H-VV using $H \to WW \to (e\nu\mu\nu)jj$

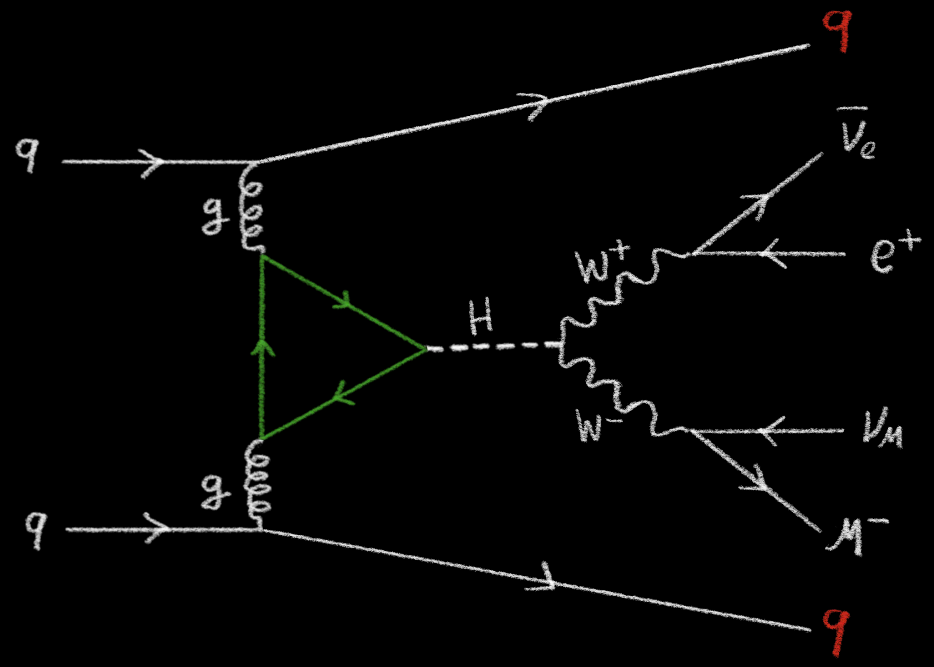

Doyeong Kim
Kansas State University

Optimal Discriminants for CP (ATLAS)

ATLAS-CONF-2020-055 | ATLAS $H \to WW \to (e\nu\mu\nu)jj$

- Optimal discriminants for ggH + 2jets topology
  - Cuts applied on kinematics of di-lepton system, and ΔR_{jj}
  - Categorize defined using $|\Delta\eta_{jj}|$ and BDTs score that trained using kinematics of di-lepton system and angular distances between leptons and jets

- Optimal discriminants for CP
  - Signed azimuthal angle difference

$$\Delta\Phi_{jj} = \begin{cases} \phi_{j_1} - \phi_{j_2} \text{ if } \eta_{j_1} > \eta_{j_2} \\ \phi_{j_2} - \phi_{j_1} \text{ otherwise} \end{cases}$$

$< \Delta\Phi_{jj} >$!= 0 would indicate CP-mixed state

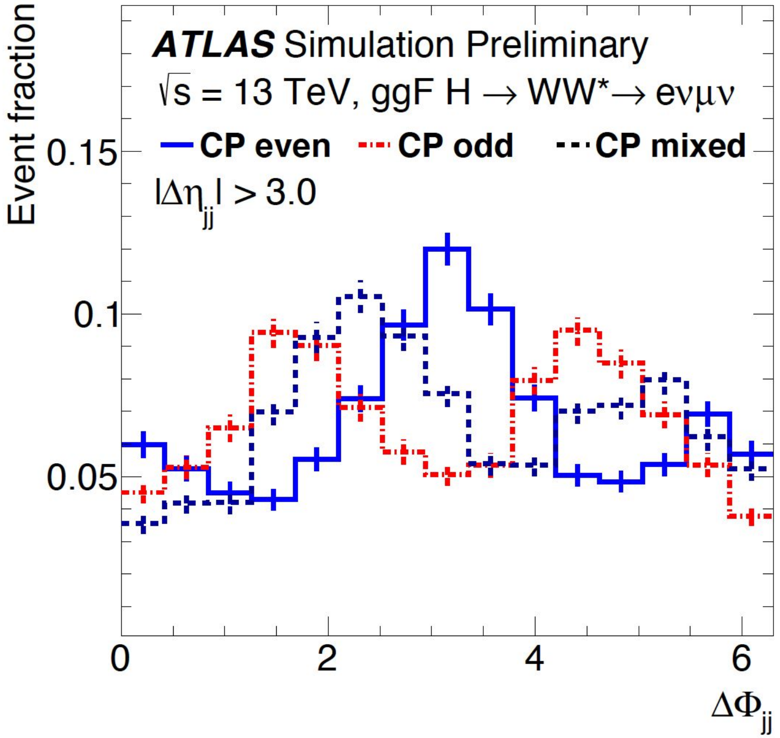

Constraint on CP-violating Parameters

ATLAS-CONF-2020-055 | ATLAS H→WW→(eνμν)jj

Using Higgs Characterisation model, CP violation in **H-VV** coupling via **ggH loop** described by

CP-even coupling strength scale factor

CP-odd coupling strength scale factor

$$\mathcal{L}_0^{\text{loop}} = -\frac{1}{4}\left(\kappa_{Hgg} g_{Hgg} G^a_{\mu\nu} G^{a,\mu\nu} + \kappa_{Agg} g_{Agg} G^a_{\mu\nu} \tilde{G}^{a,\mu\nu}\right) X_0 .$$

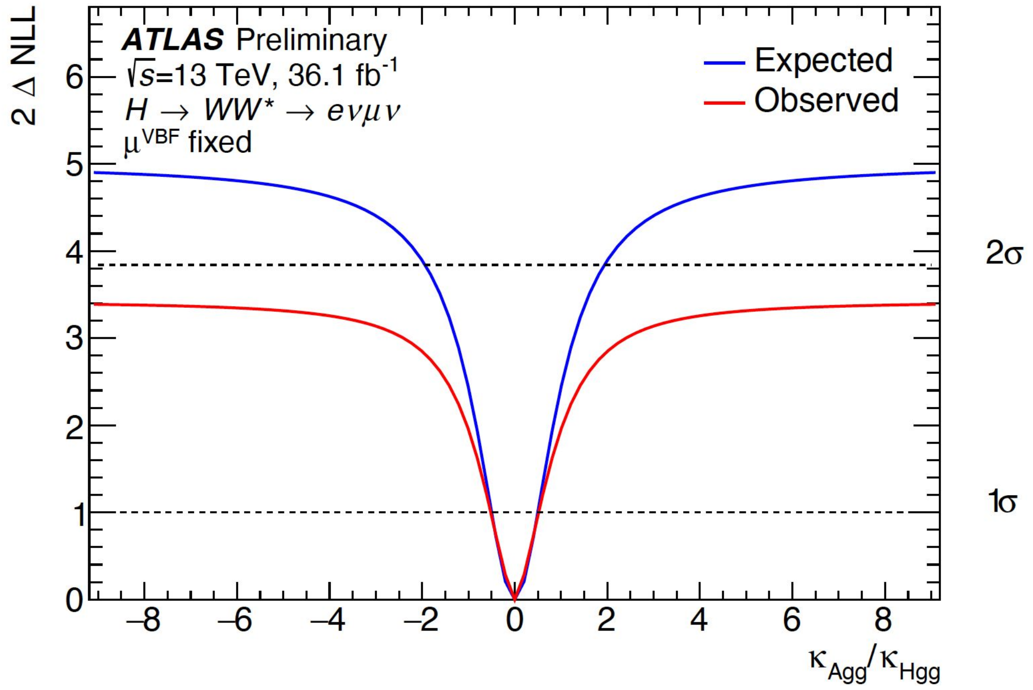

Best-fit :
0.0 ± 0.4(stat.) ± 0.3(syst.)

Good News
First measurement of polarisation effects in H-VV is also presented in this paper!

Merijn's slides (Oct 26)

Results from both experiments indicate no deviation from SM expectation

Conclusions

Conclusions

- Search for the existence of anomalous **H-VV** couplings including CP-violation is performed using three promising Higgs boson decay channels, H→ZZ→4*l*, H→WW→(eνμν)jj, and H→ττ by CMS and ATLAS collaborations
- Better precision than previous results achieved by analysing full Run2 dataset in H→ZZ→4*l*
- All measurements are consistent with the SM prediction so far, but we expect 20 times more data with future LHC runs and still plenty to explore with Higgs boson :)
  - Smaller statistical uncertainties
  - Use of other H-VV signatures (VBF H→bb, H→WW, etc)
  - Use of other vertices (H-ff)

References

[1] CMS Collaboration, "Constraints on anomalous Higgs boson couplings to vector bosons and fermions in production and decay in the H→4ℓ channel", CMS-PAS-HIG-19-009

[2] CMS Collaboration, "Constraints on anomalous HVV couplings from the production of Higgs bosons decaying to τ lepton pairs" Phys. Rev. D 100, 112002 (2019) 10.1103/PhysRevD.100.112002, arXiv:1903.06973

[3] ATLAS Collaboration, "Higgs boson production cross-section measurements and their EFT interpretation in the 4ℓ decay channel at √s = 13 TeV with the ATLAS detector", Phys. Lett. B 805 (2020) 135426, arXiv:2004.03447

[4] ATLAS Collaboration, "Test of CP invariance in vector-boson fusion production of the Higgs boson in the H→ττ channel in proton−proton collisions at √s = 13 TeV with the ATLAS detector", Phys. Lett. B 805 (2020) 135426, arXiv:2002.05315

[5] CMS Collaboration, "Constraints on anomalous Higgs boson couplings using production and decay information in the four-lepton final state", Phys. Lett. B 775 (2017) 1, arXiv:1707.00541

[6] ATLAS Collaboration, "Measurement of the Higgs boson coupling properties in the H→ZZ*→4ℓ decay channel at √s = 13 TeV with the ATLAS detector", JHEP 03 (2018) 095, arXiv:1712.02304

[7] D. de Florian et al., "Handbook of LHC Higgs cross sections: 4. deciphering the nature of the Higgs sector", CERN Report CERN-2017-002-M, 2016. doi:10.23731/CYRM-2017-002, arXiv:1610.07922

[8] ATLAS Collaboration, "Constraints on Higgs boson properties using WW*(→eνμν)jj production in 36.1 fb^{-1} of √s = 13 TeV *pp* collisions with the ATLAS detector", ATLAS-CONF-2020-055

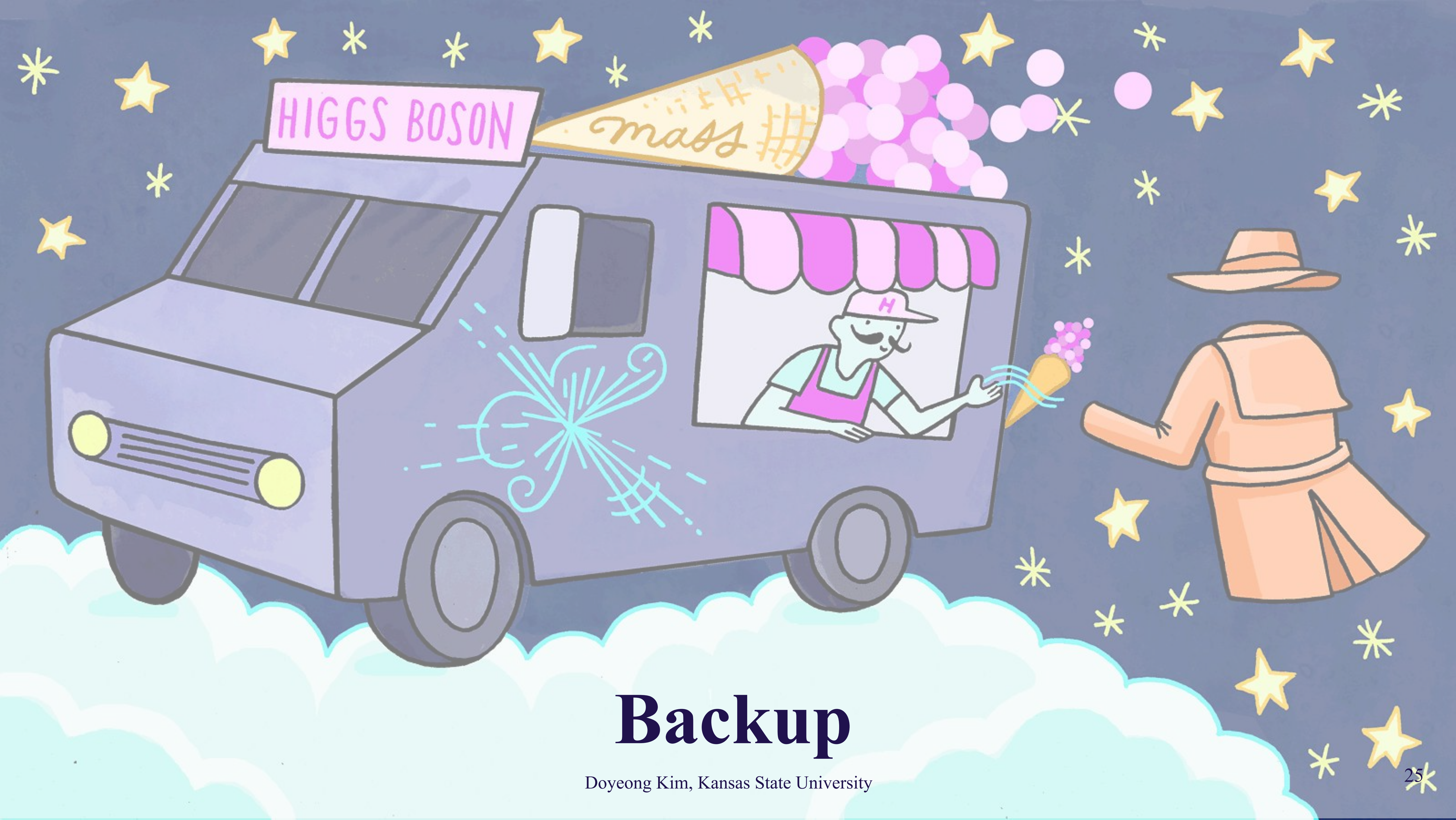

Backup

ATLAS HTT Selection & BDT Inputs

Channel	$\tau_{\mathrm{lep}}\tau_{\mathrm{lep}}$ SF	$\tau_{\mathrm{lep}}\tau_{\mathrm{lep}}$ DF	$\tau_{\mathrm{lep}}\tau_{\mathrm{had}}$	$\tau_{\mathrm{had}}\tau_{\mathrm{had}}$
Preselection	Two isolated τ-lepton decay candidates with opposite electric charge			
	$p_{\mathrm{T}}^{\tau_1} > 19^*/15^*$ GeV (μ/e)	$p_{\mathrm{T}}^{e} > 18$ GeV	$p_{\mathrm{T}}^{\tau_{\mathrm{had}}} > 30$ GeV	$p_{\mathrm{T}}^{\tau_1} > 40$ GeV
	$p_{\mathrm{T}}^{\tau_2} > 10/15^*$ GeV (μ/e)	$p_{\mathrm{T}}^{\mu} > 14$ GeV	$p_{\mathrm{T}}^{\tau_{\mathrm{lep}}} > 21^*$ GeV	$p_{\mathrm{T}}^{\tau_2} > 30$ GeV
	$m_{\tau\tau}^{\mathrm{coll}} > m_Z - 25$ GeV		$m_{\mathrm{T}} < 70$ GeV	$0.8 < \Delta R_{\tau\tau} < 2.5$
	$30 < m_{\ell\ell} < 75$ GeV	$30 < m_{\ell\ell} < 100$ GeV		$\lvert\Delta\eta_{\tau\tau}\rvert < 1.5$
	$E_{\mathrm{T}}^{\mathrm{miss}} > 55$ GeV	$E_{\mathrm{T}}^{\mathrm{miss}} > 20$ GeV		$E_{\mathrm{T}}^{\mathrm{miss}} > 20$ GeV
	$E_{\mathrm{T}}^{\mathrm{miss,\,hard}} > 55$ GeV			
	$N_{b\text{-jets}} = 0$			
VBF topology	$N_{\mathrm{jets}} \geq 2$, $p_{\mathrm{T}}^{j_2} > 30$ GeV, $m_{jj} > 300$ GeV, $\lvert\Delta\eta_{jj}\rvert > 3$			
	$p_{\mathrm{T}}^{j_1} > 40$ GeV			$p_{\mathrm{T}}^{j_1} > 70$ GeV, $\lvert\eta_{j_1}\rvert < 3.2$
BDT input variables	$m_{\tau\tau}^{\mathrm{MMC}}$, m_{jj}, $\Delta R_{\tau\tau}$, $C_{jj}(\tau_1)$, $C_{jj}(\tau_2)$, $p_{\mathrm{T}}^{\mathrm{tot}}$			
	$m_{\tau\tau}^{\mathrm{vis}}$, $m_{\mathrm{T}}^{\tau_1, E_{\mathrm{T}}^{\mathrm{miss}}}$, $p_{\mathrm{T}}^{j_3}$		$C(\phi^{\mathrm{miss}})/\sqrt{2}$	
	$\Delta\phi_{\tau\tau}$	$E_{\mathrm{T}}^{\mathrm{miss}}/p_{\mathrm{T}}^{\tau_1}$, $E_{\mathrm{T}}^{\mathrm{miss}}/p_{\mathrm{T}}^{\tau_2}$	$m_{\tau\tau}^{\mathrm{vis}}$, $\lvert\Delta\eta_{\tau\tau}\rvert$	$p_{\mathrm{T}}^{\tau\tau E_{\mathrm{T}}^{\mathrm{miss}}}$, $\lvert\Delta\eta_{\tau\tau}\rvert$
Signal region	$\mathrm{BDT}_{\mathrm{score}} > 0.78$		$\mathrm{BDT}_{\mathrm{score}} > 0.86$	$\mathrm{BDT}_{\mathrm{score}} > 0.87$

ATLAS HZZ Neural Networks Summary

Eur. Phys. J. C 80 (2020) 957 ATLAS H→ZZ→4l

Table 5: The input variables used to train the MLP, and the two RNNs for the four leptons and the jets (up to three). For each category, the processes which are classified by an NN, their corresponding input variables and the observable used are shown. For example, there are eight input variables for the Lepton RNN being trained if p_T^ℓ and η_ℓ are listed. Leptons and jets are denoted by 'ℓ' and 'j'. See the text for the definitions of the variables.

Category	Processes	MLP	Lepton RNN	Jet RNN	Discriminant
$0j$-$p_T^{4\ell}$-Low $0j$-$p_T^{4\ell}$-Med	ggF, ZZ^*	$p_T^{4\ell}$, D_{ZZ^*}, m_{12}, m_{34}, $\lvert\cos\theta^*\rvert$, $\cos\theta_1$, ϕ_{ZZ}	p_T^ℓ, η_ℓ	-	$\mathrm{NN}_{\mathrm{ggF}}$
$1j$-$p_T^{4\ell}$-Low	ggF, VBF, ZZ^*	$p_T^{4\ell}$, p_T^j, η_j, $\Delta R_{4\ell j}$, D_{ZZ^*}	p_T^ℓ, η_ℓ	-	$\mathrm{NN}_{\mathrm{VBF}}$ for $\mathrm{NN}_{ZZ} < 0.25$ NN_{ZZ} for $\mathrm{NN}_{ZZ} > 0.25$
$1j$-$p_T^{4\ell}$-Med	ggF, VBF, ZZ^*	$p_T^{4\ell}$, p_T^j, η_j, E_T^{miss}, $\Delta R_{4\ell j}$, D_{ZZ^*}, $\eta_{4\ell}$	p_T^ℓ, η_ℓ	-	$\mathrm{NN}_{\mathrm{VBF}}$ for $\mathrm{NN}_{ZZ} < 0.25$ NN_{ZZ} for $\mathrm{NN}_{ZZ} > 0.25$
$1j$-$p_T^{4\ell}$-High	ggF, VBF	$p_T^{4\ell}$, p_T^j, η_j, E_T^{miss}, $\Delta R_{4\ell j}$, $\eta_{4\ell}$	p_T^ℓ, η_ℓ	-	$\mathrm{NN}_{\mathrm{VBF}}$
$2j$	ggF, VBF, VH	m_{jj}, $p_T^{4\ell jj}$	p_T^ℓ, η_ℓ	p_T^j, η_j	$\mathrm{NN}_{\mathrm{VBF}}$ for $\mathrm{NN}_{VH} < 0.2$ NN_{VH} for $\mathrm{NN}_{VH} > 0.2$
$2j$-BSM-like	ggF, VBF	$\eta_{ZZ}^{\mathrm{Zepp}}$, $p_T^{4\ell jj}$	p_T^ℓ, η_ℓ	p_T^j, η_j	$\mathrm{NN}_{\mathrm{VBF}}$
VH-Lep-enriched	VH, ttH	N_{jets}, $N_{b\text{-jets},70\%}$, E_T^{miss}, H_T	p_T^ℓ	-	NN_{ttH}
ttH-Had-enriched	ggF, ttH, tXX	$p_T^{4\ell}$, m_{jj}, $\Delta R_{4\ell j}$, $N_{b\text{-jets},70\%}$,	p_T^ℓ, η_ℓ	p_T^j, η_j	NN_{ttH} for $\mathrm{NN}_{tXX} < 0.4$ NN_{tXX} for $\mathrm{NN}_{tXX} > 0.4$

ATLAS HWW Event Selection Summary

Table 3: Event selection criteria used to define the signal regions for the ggF + 2 jets and VBF event categories.

	ggF + 2 jets	VBF
Preselection	Two isolated, different-flavour leptons ($\ell = e, \mu$) with opposite charge $p_T^{lead} > 22$ GeV, $p_T^{sublead} > 15$ GeV $m_{\ell\ell} > 10$ GeV $N_{jet} \geq 2$	
Background rejection	$N_{b-jet,(p_T>20\text{ GeV})} = 0$ $m_{\tau\tau} < 66$ GeV	
	$\Delta R_{jj} > 1.0$ $p_{T,\ell\ell} > 20$ GeV $m_{\ell\ell} < 90$ GeV $m_T < 150$ GeV	central jet veto outside lepton veto
BDT input variables	$m_{\ell\ell}, m_T, p_{T,\ell\ell}, \Delta\phi_{\ell\ell}$ $\min \Delta R(\ell_1, j_i), \min \Delta R(\ell_2, j_i)$	$m_{jj}, \Delta Y_{jj}, m_{\ell\ell}, m_T, \Delta\phi_{\ell\ell}$ $\sum_\ell C_\ell, \sum_{\ell,j} m_{\ell,j}, p_T^{tot}$

CMS H→ZZ→4l Categorization

CMS-PAS-HIG-19-009 | CMS H→ZZ→4l

Table 3: The numbers of events expected in the SM for different H signal (sig.) and background (bkg.) contributions and the observed number of events in each category defined in Scheme 2 targeting HVV anomalous couplings. The EW (VBF, WH, and ZH) signal expectation is quoted for the SM and anomalous ($a_3/a_2/\kappa_1/\kappa_2^{Z\gamma}$) scenarios, all generated with the same total EW production cross section.

	Untagged	Boosted	VBF-1jet	VBF-2jet	VH-leptonic	VH-hadronic
ggH sig.	175.2	6.7	14.6	9.5	0.4	5.7
VBF sig. ($a_3/a_2/\kappa_1/\kappa_2^{Z\gamma}$)	5.7 (0.3/0.4/0.1/0.1)	1.4 (1.0/0.8/0.6/0.5)	2.7 (0.1/0.1/0.0/0.1)	7.6 (5.5/4.4/1.7/1.5)	0.1 (0.0/0.0/0.0/0.0)	0.5 (0.3/0.2/0.1/0.1)
WH sig. ($a_3/a_2/\kappa_1/\kappa_2^{Z\gamma}$)	2.3 (2.1/3.3/0.7/0.0)	0.5 (4.0/3.4/6.4/0.0)	0.3 (0.8/0.9/0.2/0.0)	0.2 (1.0/0.9/1.7/0.0)	1.1 (2.8/2.9/3.4/0.0)	1.1 (3.1/3.0/2.6/0.0)
ZH sig. ($a_3/a_2/\kappa_1/\kappa_2^{Z\gamma}$)	2.4 (1.3/2.4/0.9/1.3)	0.4 (2.4/2.1/5.1/13.5)	0.2 (0.4/0.4/0.2/0.3)	0.2 (0.6/0.6/1.4/3.8)	0.3 (0.5/0.6/0.8/2.0)	0.9 (1.6/1.7/2.0/4.6)
$b\bar{b}$H sig.	1.9	0.0	0.1	0.1	0.0	0.1
$t\bar{t}$H sig.	1.4	0.0	0.0	0.5	0.2	0.2
Signal expected ($a_3/a_2/\kappa_1/\kappa_2^{Z\gamma}$)	188.8 (182.1/184.5/180.2/179.9)	9.2 (14.3/13.0/18.9/20.9)	17.9 (16.1/16.2/15.1/15.1)	18.1 (17.3/16.0/15.0/15.4)	2.2 (4.0/4.2/4.9/2.7)	8.6 (11.1/11.0/10.8/10.7)
$q\bar{q} \to 4\ell$ bkg.	212.8	2.0	6.5	2.4	2.4	2.2
$gg \to 4\ell$ bkg.	20.0	0.0	1.2	0.3	0.4	0.1
Z + X bkg.	68.2	3.8	2.3	8.2	1.1	3.8
Total expected	489.8 (483.1/485.5/481.1/480.9)	15.0 (20.1/18.9/24.7/26.7)	28.0 (26.1/26.2/25.2/25.1)	29.0 (28.2/26.9/25.9/26.3)	6.1 (7.9/8.0/8.8/6.6)	14.7 (17.1/17.0/16.8/16.7)
Total observed	503	17	26	21	8	14

- The VBF-2jet category requires exactly four leptons, either two or three jets of which at most one is b-quark flavor-tagged, or more if none are b-tagged jets, and max $\left(\mathcal{D}_{2jet}^{VBF,i}\right) > 0.5$ using either the SM or any of the four BSM signal hypotheses (i) for the VBF production. See Fig. 1 (left) for illustration.
- The VH-hadronic category requires exactly four leptons, either two or three jets, or more if none are b-tagged jets, and max $\left(\mathcal{D}_{2jet}^{WH,i}, \mathcal{D}_{2jet}^{ZH,i}\right) > 0.5$ using either the SM or any of the four BSM signal hypotheses (i) for the VH production. See Fig. 1 (right) for illustration.
- The VH-leptonic category requires no more than three jets and no b-tagged jets in the event, and exactly one additional lepton or one additional pair of opposite sign same flavor leptons. This category also includes events with no jets and at least one additional lepton.
- The VBF-1jet category requires exactly four leptons, exactly one jet and $\mathcal{D}_{1jet}^{VBF} > 0.7$.
- The Boosted category requires exactly four leptons, three or fewer jets, or more if none are b-tagged jets, and the transverse momentum of the four-lepton system $p_T^{4\ell} > 120$ GeV.
- The Untagged category consists of the remaining events.

CMS HZZ Observables

Category	Selection	Observables $\vec{x}$ for fitting
Untagged	none below	$\mathcal{D}_{\rm bkg}, \mathcal{D}_{0-}^{\rm dec}, \mathcal{D}_{0h+}^{\rm dec}, \mathcal{D}_{\Lambda1}^{\rm dec}, \mathcal{D}_{\Lambda1}^{Z\gamma,\rm dec}, \mathcal{D}_{\rm CP}^{\rm dec}, \mathcal{D}_{\rm int}^{\rm dec}$
Boosted	$p_{\rm T}^{4\ell} > 120$ GeV	$\mathcal{D}_{\rm bkg}, p_{\rm T}^{4\ell}$
VBF-1jet	$\mathcal{D}_{\rm 1jet}^{\rm VBF} > 0.7$	$\mathcal{D}_{\rm bkg}, p_{\rm T}^{4\ell}$
VBF-2jet	$\mathcal{D}_{\rm 2jet}^{\rm VBF} > 0.5$	$\mathcal{D}_{\rm bkg}, \mathcal{D}_{0-}^{\rm VBF+dec}, \mathcal{D}_{0h+}^{\rm VBF+dec}, \mathcal{D}_{\Lambda1}^{\rm VBF+dec}, \mathcal{D}_{\Lambda1}^{Z\gamma,\rm VBF+dec}, \mathcal{D}_{\rm CP}^{\rm VBF}, \mathcal{D}_{\rm int}^{\rm VBF}$
VH-leptonic	see Sec. 3	$\mathcal{D}_{\rm bkg}, p_{\rm T}^{4\ell}$
VH-hadronic	$\mathcal{D}_{\rm 2jet}^{\rm VH} > 0.5$	$\mathcal{D}_{\rm bkg}, \mathcal{D}_{0-}^{\rm VH+dec}, \mathcal{D}_{0h+}^{\rm VH+dec}, \mathcal{D}_{\Lambda1}^{\rm VH+dec}, \mathcal{D}_{\Lambda1}^{Z\gamma,\rm VH+dec}, \mathcal{D}_{\rm CP}^{\rm VH}, \mathcal{D}_{\rm int}^{\rm VH}$

Constraint on Wilson Coefficients

Eur. Phys. J. C 80 (2020) 957 | ATLAS H→ZZ→4l

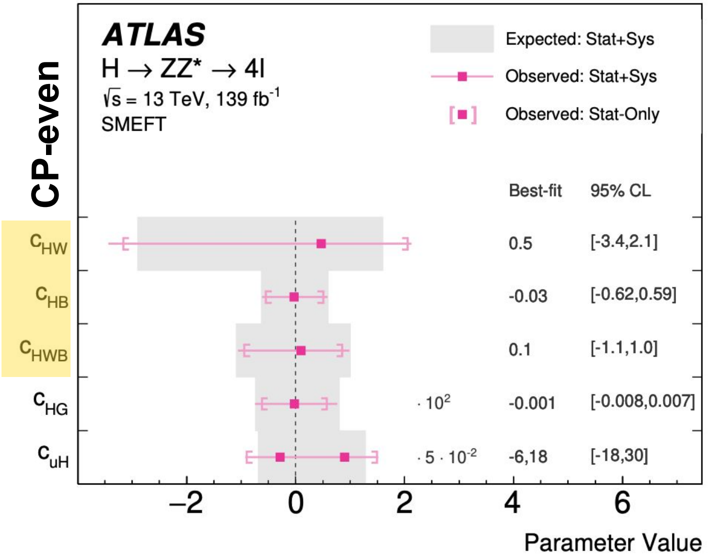

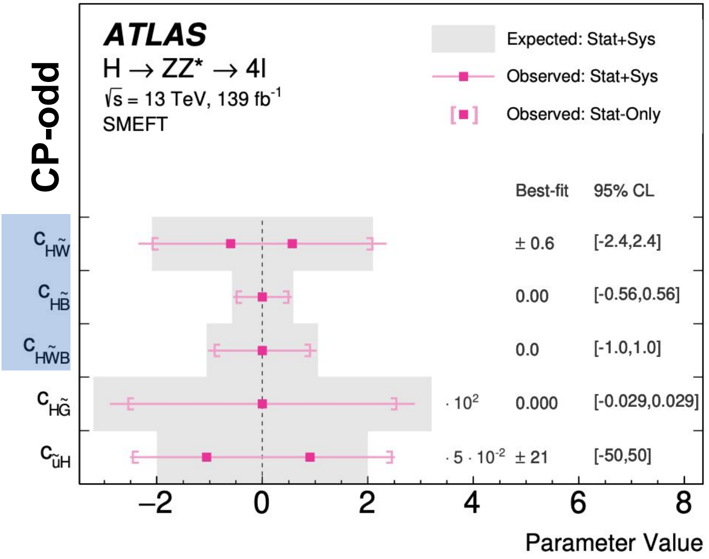

- One Wilson coefficient fitted at a time
- Following the constraint on CHG the next-strongest constraints are obtained on H-VV related coefficients
  - Driving contribution is from ggH production **decay to ZZ**
  - **VBF and VH productions** also give some sensitivity

Primary contribution to H-VV vertices

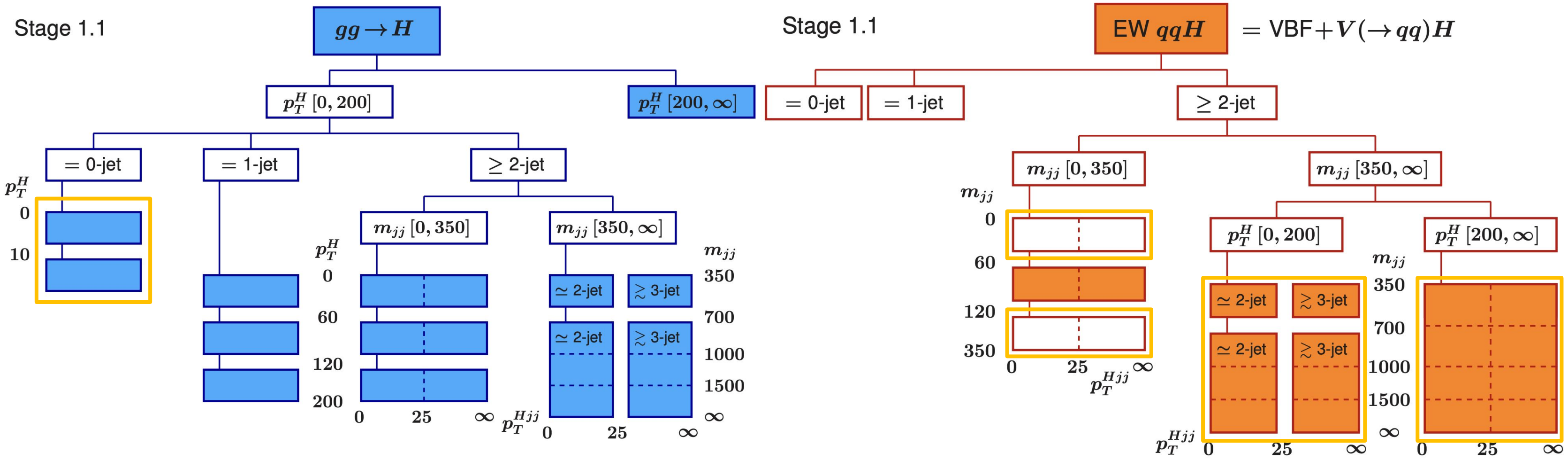

STXS Stage 1.2 Bins

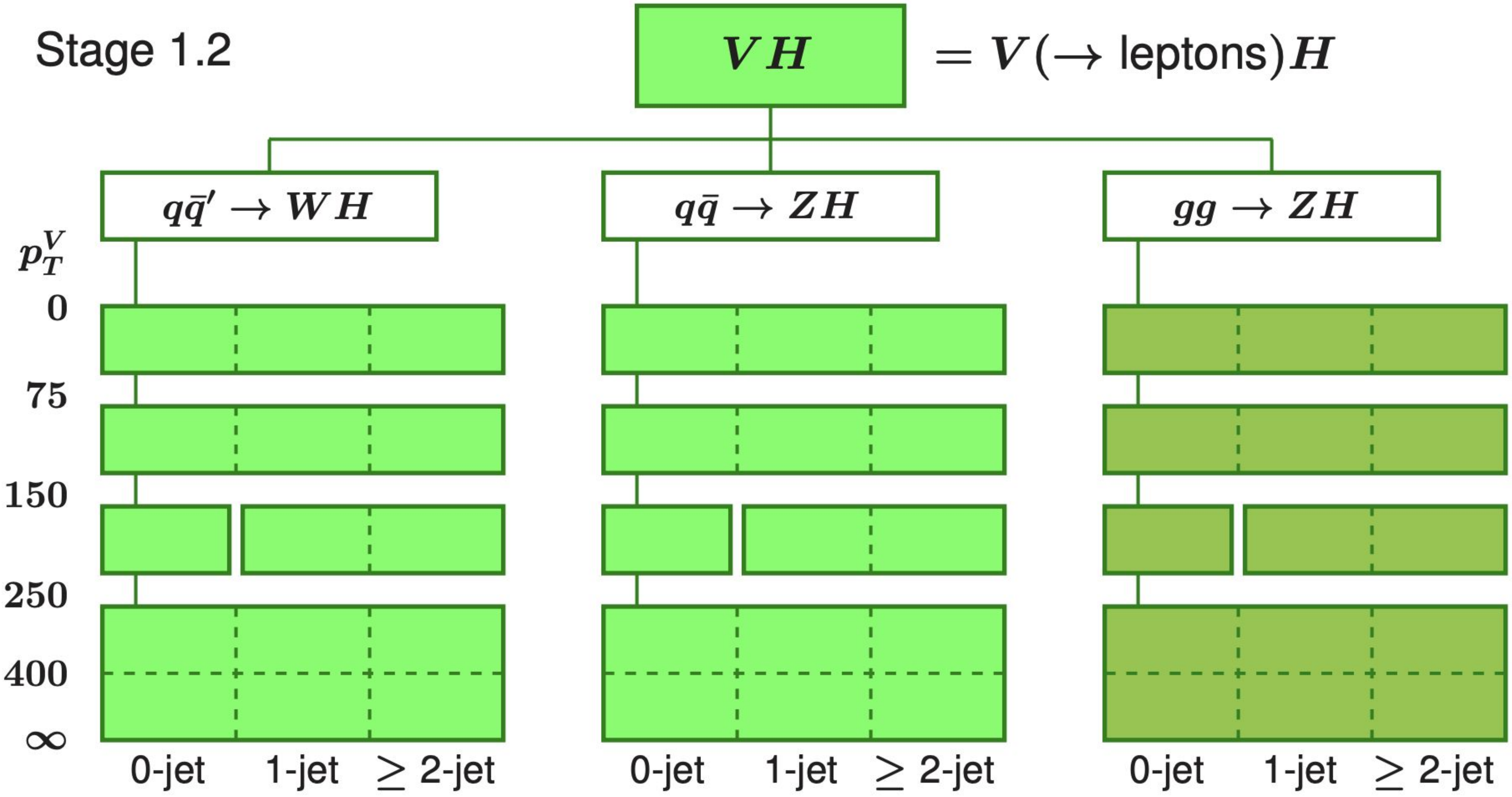

CP studies using H-VV

Constraint on H-VV Couplings (CMS)

CMS-PAS-HIG-19-009 | CMS H→ZZ→4*l*

Coupling Amplitude Decomposition

SMEFT (Higgs basis)

a_3 (CP-odd)

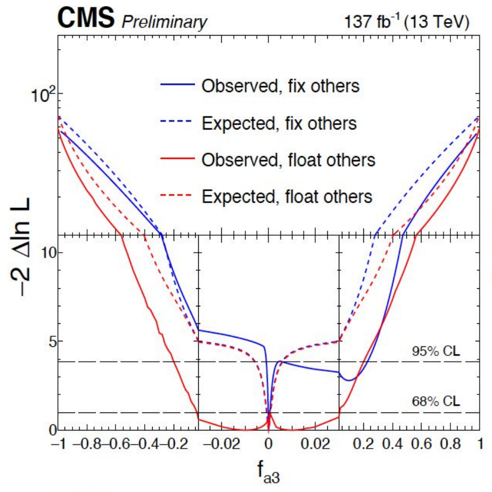

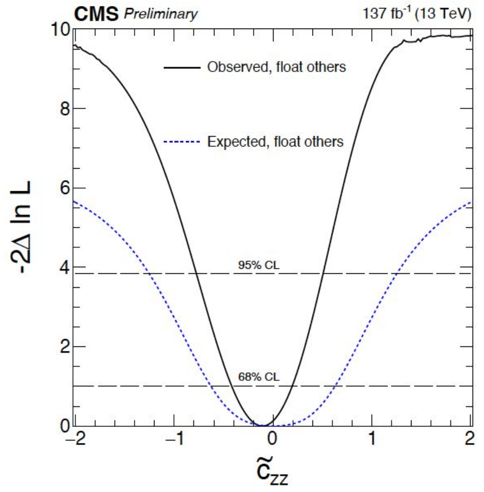

a_2 (CP-even)

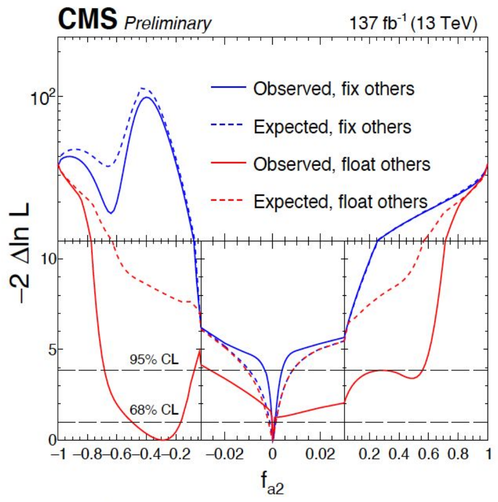

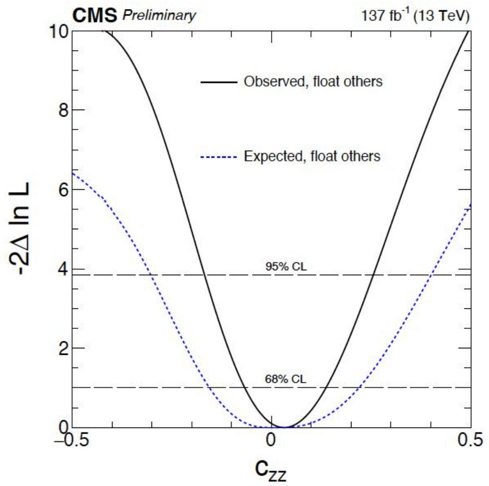

- Results are shown in terms of
  1) Coupling amplitude decomposition
  2) SMEFT represented in Higgs basis
- All anomalous couplings measured simultaneously

Limits of other parameters are in backup

Constraint on H-VV Couplings (CMS)

Phys. Rev. D 100, 112002 | CMS H→$\tau\tau$

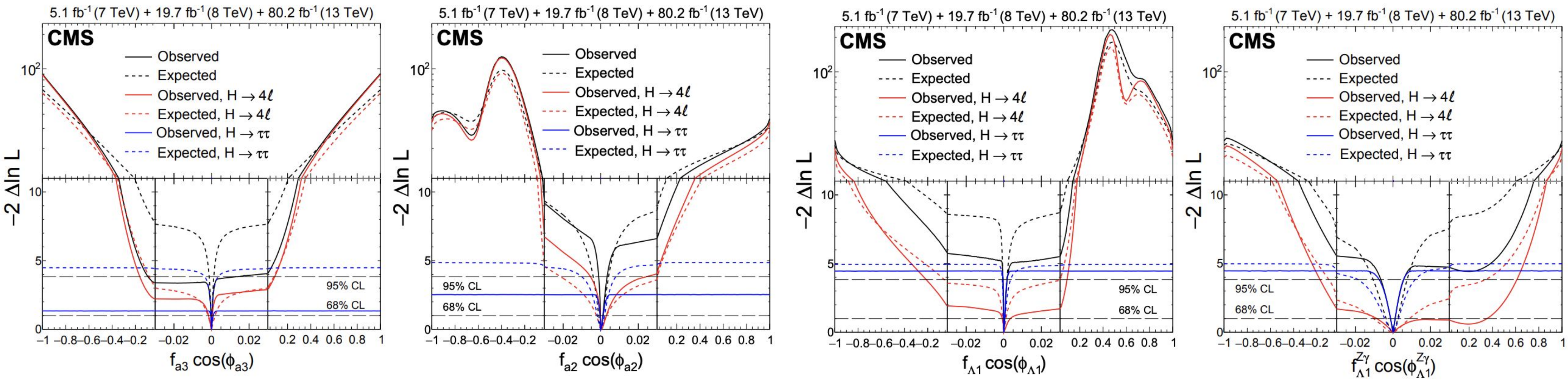

Combination of H→$\tau\tau$ (Run2 2016) and H→4l (Run1 2011, 2012 and Run2 2015, 2016, 2017)

Effective XS Fraction and Phase

Generic spin-0 HVV scattering amplitude

$$A(\mathrm{HVV}) \sim \left[a_1^{\mathrm{VV}} + \frac{\kappa_1^{\mathrm{VV}} q_1^2 + \kappa_2^{\mathrm{VV}} q_2^2}{\left(\Lambda_1^{\mathrm{VV}}\right)^2} \right] m_{\mathrm{V1}}^2 \epsilon_{\mathrm{V1}}^* \epsilon_{\mathrm{V2}}^* + a_2^{\mathrm{VV}} f_{\mu\nu}^{*(1)} f^{*(2)\mu\nu} + a_3^{\mathrm{VV}} f_{\mu\nu}^{*(1)} \tilde{f}^{*(2)\mu\nu}$$

tree level scalar (0^+) | higher order scalar (0^+_h) | pseudoscalar (0^-)

Coupling parameters

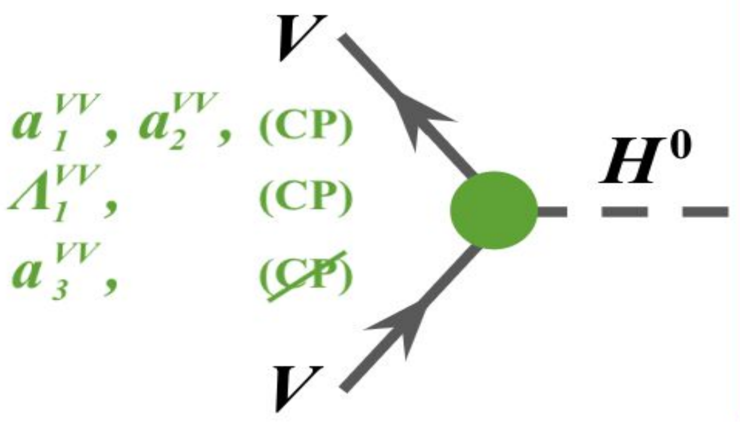

$$f_{a3} = \frac{|a_3|^2\sigma_3}{|a_1|^2\sigma_1 + |a_2|^2\sigma_2 + |a_3|^2\sigma_3 + \tilde{\sigma}_{\Lambda 1}/\left(\Lambda_1\right)^4 + \dots}, \quad \phi_{a3} = \arg\left(\frac{a_3}{a_1}\right),$$

$$f_{a2} = \frac{|a_2|^2\sigma_2}{|a_1|^2\sigma_1 + |a_2|^2\sigma_2 + |a_3|^2\sigma_3 + \tilde{\sigma}_{\Lambda 1}/\left(\Lambda_1\right)^4 + \dots}, \quad \phi_{a2} = \arg\left(\frac{a_2}{a_1}\right),$$

$$f_{\Lambda 1} = \frac{\tilde{\sigma}_{\Lambda 1}/\left(\Lambda_1\right)^4}{|a_1|^2\sigma_1 + |a_2|^2\sigma_2 + |a_3|^2\sigma_3 + \tilde{\sigma}_{\Lambda 1}/\left(\Lambda_1\right)^4 + \dots}, \quad \phi_{\Lambda 1},$$

$$f_{\Lambda 1}^{Z\gamma} = \frac{\tilde{\sigma}_{\Lambda 1}^{Z\gamma}/\left(\Lambda_1^{Z\gamma}\right)^4}{|a_1|^2\sigma_1 + \tilde{\sigma}_{\Lambda 1}^{Z\gamma}/\left(\Lambda_1^{Z\gamma}\right)^4 + \dots}, \quad \phi_{ai}^{Z\gamma},$$

- Advantage of measuring the effective cross-section ratios
  - Many systematics can be canceled out
  - Parameter range is conveniently confined from 0 to 1
- Value $\mathbf{0 < |f_{a3}| < 1}$ would indicate CP violation → **BSM!**

Parametrization of Scattering Amplitudes

Generic spin-0 HVV scattering amplitude

tree-level SM-like

$$\mathcal{A}(\mathrm{HVV}) \sim \left[a_1^{VV} + \frac{\kappa_1^{VV} q_1^2 + \kappa_2^{VV} q_2^2}{\left(\Lambda_1^{VV}\right)^2} \right] m_{V1}^2 \epsilon_{V1}^* \epsilon_{V2}^* + a_2^{VV} f_{\mu\nu}^{*(1)} f^{*(2)\mu\nu} + a_3^{VV} f_{\mu\nu}^{*(1)} \tilde{f}^{*(2)\mu\nu}$$

$a_1^{ZZ} = a_1^{WW}$ (custodial symmetry)

Where VV = ZZ, WW, $Z\gamma$, $\gamma\gamma$ or gg

Considering gauge invariance

1) When VV = ZZ, WW, $Z\gamma$ — 4 couplings from each term

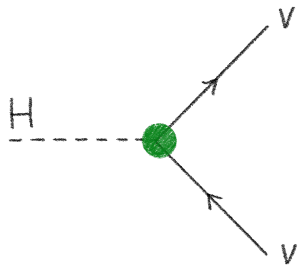

- a_1^{VV} (CP) : SM, where $a_1^{Z\gamma} = 0$
- a_2^{VV} (CP)
- Λ_1^{VV} (CP)
- a_3^{VV} ~~(CP)~~

2) When VV = $\gamma\gamma$, gg — 2 couplings from 3rd and 4th terms

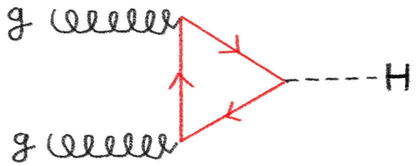

- a_2^{VV} (CP) : SM
- a_3^{VV} ~~(CP)~~

In total, 15 couplings

- 4 constraint

  $a_i^{ZZ} = a_i^{WW}$, $\kappa_i^{ZZ}/(\Lambda_1^{ZZ})^2 = \kappa_i^{WW}/(\Lambda_1^{WW})^2$

  Hereafter WW and ZZ superscript will be omitted

- 4 uninteresting couplings

  Earlier measurement indicates substantially tighter limits on $a_2^{\gamma\gamma/Z\gamma}$, $a_3^{\gamma\gamma/Z\gamma}$

---

2 SM-like couplings :

→ $\mathbf{a_1}$ and $\mathbf{a_2^{ggH}}$

5 anomalous couplings are of our interest :

→ $\mathbf{a_2}$, $\mathbf{a_3}$, $\mathbf{\Lambda_1}$, $\mathbf{\Lambda_1^{Z\gamma}}$ and $\mathbf{a_3^{ggH}}$